DETERMINATION OF SEISMIC SOURCE DEPTHS FROM DIFFERENTIAL TRAVEL TIMES

ENSCO, Incorporated

PREPARED FOR
Air Force Technical Applications Center

30 June 1975

add. 6

225223

ADA028035

ENSCO, INC.
Information & System Sciences Division
8001 Forbes Place
Springfield, Virginia 22151
Phone: (703) 569-9000

DEPARTMENT OF DEFENSE FORMS

F-200.1473 *DD Form 1473:* Report Documentation Page

SECURITY CLASSIFICATION OF THIS PAGE (When Data Entered)

REPORT DOCUMENTATION PAGE		READ INSTRUCTIONS BEFORE COMPLETING FORM
1. REPORT NUMBER	2. GOVT ACCESSION NO	3. RECIPIENT'S CATALOG NUMBER
4. TITLE (and Subtitle) Determination of Seismic Source Depths from Differential Travel Times		5. TYPE OF REPORT & PERIOD COVERED Final Report 6. PERFORMING ORG. REPORT NUMBER N/A
7. AUTHOR(s) Edward Page, Robert Bauman		8. CONTRACT OR GRANT NUMBER(s) F08606-75-C-0025
9. PERFORMING ORGANIZATION NAME AND ADDRESS ENSCO, INC. 8001 Forbes Pl., Spfld, Va.		10. PROGRAM ELEMENT, PROJECT, TASK AREA & WORK UNIT NUMBERS
11. CONTROLLING OFFICE NAME AND ADDRESS DCASD, Baltimore Bld. 22, Fort Holabird, Baltimore, Maryland 21219		12. REPORT DATE 30 June 1975 13. NUMBER OF PAGES 59
14. MONITORING AGENCY NAME & ADDRESS (if different from Controlling Office) VELA Seismological Center 312 Montgomery Street Alexandria, Virginia 22314		15. SECURITY CLASS (of this report) 15A. DECLASSIFICATION/DOWNGRADING SCHEDULE

16. DISTRIBUTION STATEMENT (of this Report)

APPROVED FOR PUBLIC RELEASE
DISTRIBUTION UNLIMITED

17. DISTRIBUTION STATEMENT (of the abstract entered in Block 20, if different from Report)

18. SUPPLEMENTARY NOTES

19. KEY WORDS (Continue on reverse side if necessary and identify by block number)

Seismic depth, depth phase, echo detection

20. ABSTRACT (Continue on reverse side if necessary and identify by block number)

New analysis techniques, developed for the detection of seismic depth phases, have been applied to three seismic events. These techniques were shown to greatly enhance the analyst's ability to determine seismic source depths.

DD FORM 1 JAN 73 1473 EDITION OF 1 NOV 65 IS OBSOLETE **PRICES SUBJECT TO CHANGE**

SECURITY CLASSIFICATION OF THIS PAGE (When Data Entered)

DETERMINATION OF SEISMIC SOURCE DEPTHS FROM DIFFERENTIAL TRAVEL TIMES

FINAL REPORT

Edward A. Page
Robert W. Bauman

July 1975

Sponsored by:

Advanced Research Project Agency
ARPA Order No. 1620

Notice of Disclaimer

The views and conclusions contained in this document are those of the author and should not be interpreted as necessarily representing the official policies, either expressed or implied, of the Advanced Research Projects Agency, the Air Force Technical Applications Center, or the U. S. government.

SUBJECT: Determination of Seismic Source Depths from Differential Travel Times

AFTAC Project No----------VELA T/5710

ARPA Order No----------2551

ARPA Program Code No----------5F10

Name of Contractor----------ENSCO, INC.

Contract Number----------F0806-75-C-0025

Effective Date of Contract----------1 November 1974

Report Period----------November 1, 1975 to June 30, 1975

Amount of Contract----------$49,791

Contract Expiration Date----------30 June 1975

Project Scientist----------Edward Page (703) 569-9000

TABLE OF CONTENTS

1.0 INTRODUCTION

The objective of this research effort was to further investigate the applicability of statistical signal processing techniques developed during the previous contract (Contract # F08606-74-C-0020) for the purpose of enhancing seismic source depth determinations. These techniques were designed to improve the detection and interpretation of seismic depth phase information contained throughout the seismogram. Three seismic events were analyzed during this contract period, and the results obtained clearly demonstrated the ability of these new depth phase detection techniques to obtain seismic source depths for events in which conventional analysis was ineffective.

The primary interest in improving seismic depth phase detection is that depth phase information gives reliable estimates of seismic source depths. Source depth is a critical factor in the discrimination between man-made events and natural seismic events since the maximum depth of burial for man-made events is of the order of ten kilometers and earthquakes can originate at much greater depths.

At present, depth phase detection is performed by analyzing the first arrival portion of the seismogram for the presence of the pP and sP arrivals. Analysis is usually done through attempts to visually identify the pP and sP first movements from seismograms recorded over a suite of stations. Identification of the depth phase is verified when the variations in the differential travel times are in agreement with the differential travel time tables for the given source to station differences. Correlation techniques are also applied to first arrival

portions of seismograms in an effort to detect the presence of the depth phases and their delay times. Both of these detection methods use only the first arrival portion of the seismogram containing the pP and sP first movements and ignore the abundance of depth phase information contained in the direct and surface reflected waveforms present throughout the entire seismogram. Ignoring this additional depth information limits the inherent detectability of these methods.

Our efforts have focused on the development of a cepstral estimation procedure which makes constructive use of the depth phase information present throughout the seismograms recorded over a suite of stations. This analysis is based on techniques which account for the depth phase delay time variations associated with the later seismic arrivals and on a technique which utilizes the phase differences between the direct and surface reflected arrivals in order to enhance the detection of depth phases. A Cepstrum Matched Filter technique was developed to aid in interpreting the typically complicated cepstral patterns resulting from this analysis. It has proven to be very valuable in further improving seismic depth phase detection.

Based on the work done to date, all indications are that these new seismic depth phase detection techniques will greatly enhance the analyst's ability to determine seismic source depths.

2.0 DEPTH PHASE ANALYSIS TECHNIQUES

The most accurate estimates of teleseismic source depths are obtained through the measurement of the differential travel times between the direct seismic arrival (P wave) and the surface reflected arrivals (pP and sP). The pP phase follows the P phase by roughly 1/4 second for each kilometer of source depth, and the sP phase follows the P phase by about 1/3 second per kilometer of depth. Therefore, by obtaining estimates of P-pP or P-sP delay times to within 1/3 second, it is possible to estimate the source depth to within one or two kilometers. Depth estimates of this accuracy are extremely useful in distinguishing natural events from man-made events. The present difficulty in using depth phase information to determine source depths is that the depth phases are identified for only about half the events analyzed using the conventional techniques.

Depth phase detection is generally performed by visual identification of the P, pP, and sP first movements (See Figure 1). Identifications of the depth phases are verified when the variations in the differential travel times are in agreement with the differential travel time tables for the given source to station distances. Both the detectability and accuracy of these delay time estimates are limited in this procedure since both are based on identifying the P, pP, or sP first movements. Correlation techniques are sometimes used to analyze the first arrival portion of the seismogram (that portion containing the P, pP, and sP first arrivals) for the presence of the pP and sP phases. However, both of these detection techniques have limited detectability and resolution since they use depth

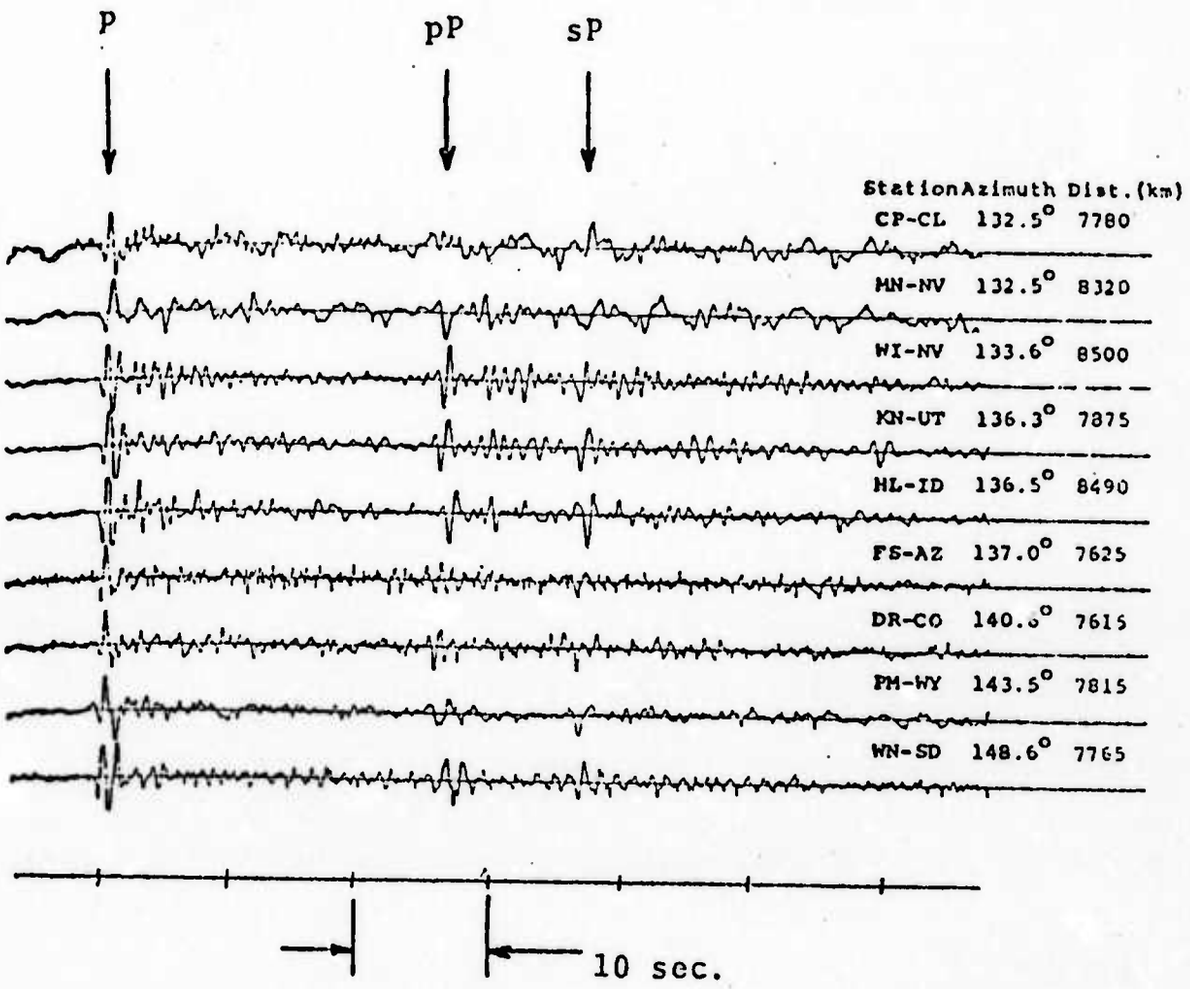

Figure 1. An Example of Unfiltered Z-Component Seismograms showing Initial Phases (Bolivia Event 12:02:22 Z 19 July 1962).

phase information contained only in the first arrival portion of the seismogram and ignore the abundance of depth phase information contained in the direct and surface reflected waveforms present throughout the rest of the seismogram.

In the following section, we discuss statistical techniques for utilizing depth phase information contained in the entire seismogram. These techniques are Stochastic Cepstrum Stacking and Stochastic Cesptrum Phasor Stacking.

2.1 Statistical Techniques for Utilizing Depth Phase Information Contained in the Coda

In order to constructively use the depth phase information contained in the seismic coda, one must be aware of variations in the depth phase delay times observed along the coda. The largest of these variations originate from the differential travel times between later seismic arrivals such as PP, PcP, PPP, etc and their associated surface reflections pPP, sPP, pPcP, sPcP, pPPP, sPPP, etc. Other contributions to the delay time variations include background noise, multipath effects, and differential distortions in the seismic waveforms caused by the properties of the medium. A cepstrum estimation procedure that allows for these delay time variations has proven to be very useful. As described in Appendix A, "Stochastic Cepstrum Stacking," this procedure allows for these delay time variations by stochastically averaging cepstra calculated from different portions of the seismogram to enable improved detection of pP-P time delays. With conventional averaging of these cepstra, detectability is significantly reduced.

In many cases, further enhancement in depth phase detectability is achieved by utilizing the relative phase difference between the direct and surface reflected seismic arrivals. In Appendix B, "Stochastic Cepstrum Phasor Stack," we show that the phase of the cosinusoidal modulation of the power spectrum resulting from the presence of the delayed surface reflected arrival can be assigned to each cepstrum amplitude and these values can then be treated as cepstrum phasors. These phase angles can be used to help distinguish cepstrum peaks resulting from surface reflected arrivals from those resulting from spurious sources.

Both the Stochastic Cepstrum Stack and Stochastic Cepstrum Phasor Stack techniques were used in the analysis of events during this contract. The results are given in Section 3. The detailed mathematical description of the steps involved in computing these cepstra is described in Appendix C.

In the next section, we discuss a Cepstrum Matched Filter technique which was developed as an aid to interpretating the depth phase information contained in these computed cepstra.

2.2 Cepstrum Matched Filter Technique

The previous sections described techniques which enable one to utilize the depth phase information contained in the seismic coda and thereby enhance the appearance of the cepstrum peak corresponding to the pP-P delay time. If one can identify such a cepstrum peak, the source depth can then be accurately determined from differential travel time tables, provided the velocity versus depth assumptions are valid. However, cepstrum peaks corresponding to the pP-P time delay τ_1, the sP-P time delay τ_2, as well as the sP-pP time delay, will in general result from a single seismic source. According th the particular cepstrum algorithm used, additional peaks will appear at $n\tau_1 \pm m\tau_2$ (where n and m are integers) when non-linear operations are included in the cepstrum computation. Thus, there is in general a complicated set of cepstral peaks corresponding to a single source depth. In this section, we describe the Cepstrum Matched Filter (CMF) technique, which is an automatic method of recognizing the presence of a cepstrum pattern corresponding to a particular source depth, over a range of possible source depths.

If one assumes that the cepstral peaks appearing at the pP-P, sP-P and sP-pP time delays dominate the expected cepstrum pattern for an event, then one can formulate the CMF algorithm in the following way. Consider the cepstrum to consist of N amplitude values CP(n) for the time delays $t_n=(n-1)\cdot\Delta t$, where $n = 1,2,3...N$. Then the synthetic cepstrum (CS) expected for an event at a given depth and distance corresponding to a pP-P delay time of τ, can be represented by:

$$CS(n,\tau,\alpha) = Q(n,(\alpha-1)\tau) + Q(n,\tau) + Q(n,\alpha\tau)$$

with $\alpha = T_{sP-p}/T_{pP-p}$, and is the ratio of delay times for sP-P and pP-P. Also Q is defined by

$$Q(n,\tau) = 1 \; ; \text{ if } \; \tau-\Delta t<t_n<\tau+\Delta t \, ,$$
$$= 0 \; ; \text{ otherwise} .$$

Thus, CS is represented by three unit amplitude peaks located at the sP-pP, pP-P, and sP-P delay times, each peak consisting of three adjacent delay time points.

The CMF output at time delay τ is defined to be the maximum zero lag correlation of the computed cepstrum (CP) with the synthesized cepstrum (CS) for a source depth having a pP-P delay time τ computed over a range of ratios α. This can be written as

$$CMF(\tau) = \max_{\alpha_1 \le \alpha \le \alpha_2} \left\{ \sum_{n=1}^{N} CP(n)\cdot CS(n,\tau,\alpha) \right\} \; ; \; \begin{array}{l} \text{if } CP(\tau)>.7\cdot CP(\alpha\tau) \\ \text{and } CP(\tau)>.7\cdot CP((\alpha-1)\tau) \end{array}$$

$$= CP(\tau) \; ; \text{ otherwise}$$

Here, α_1 and α_2 are set from the expected range of values for α for a given range of possible depths. Values of $\alpha_1 = 1.25$ and $\alpha_2 = 1.55$ were used for the event distances and depths encountered in this research. The constraints imposed require that the amplitude of the cepstrum peak at τ must be at least .7 times the amplitude of the cepstrum peaks at both $\alpha\tau$ and $(\alpha-1)\tau$. This eliminates detection of cepstral patterns for cases in

which the strength of the pP arrival is considerably less than that of the sP arrival. Thus, a cepstrum peak at τ resulting from a pP arrival for an event will not contribute to the CMF output for an apparent event having an expected sP-P delay time of τ, without the significant presence of a pP arrival for this apparent event.

As an example of the application of this technique, consider Figure 2. At the top of the figure is the cepstrum calculated from an event of known depth having both the pP and sP depth phases clearly identifiable. This cepstrum pattern is dominated by three peaks corresponding to the sP-pP, pP-P, and sP-P delay times. Upon interpreting this cepstrum for an unknown event depth, one sees that each of the three peaks has the possibility of corresponding to the pP phase. The CMF output is plotted at the bottom of Figure 2 and indicates a much stronger emphasis on the peak corresponding to the correct pP-P delay time for this event. This result reflects the fact that this cepstrum pattern primarily consisting of three peaks is in strong agreement with the pattern expected for a single event having this pP-P delay time. The lesser probability that the relative location of these three peaks was coincidental, and that one of the other two peaks actually corresponded to the correct pP-P delay time, is indicated by the presence of CMF output peaks at those delay times having reduced amplitudes.

Another example of the usefulness of the CMF is shown in Figure 3. At the top of this figure is a cepstrum calculated for the same event, but using data recorded at a single station. The figure contains four cepstrum peaks having approximately equal amplitudes making the interpretation of the source depth difficult. At the bottom of the figure is the CMF interpretation of this cepstrum which reveals a strong emphasis on the peak

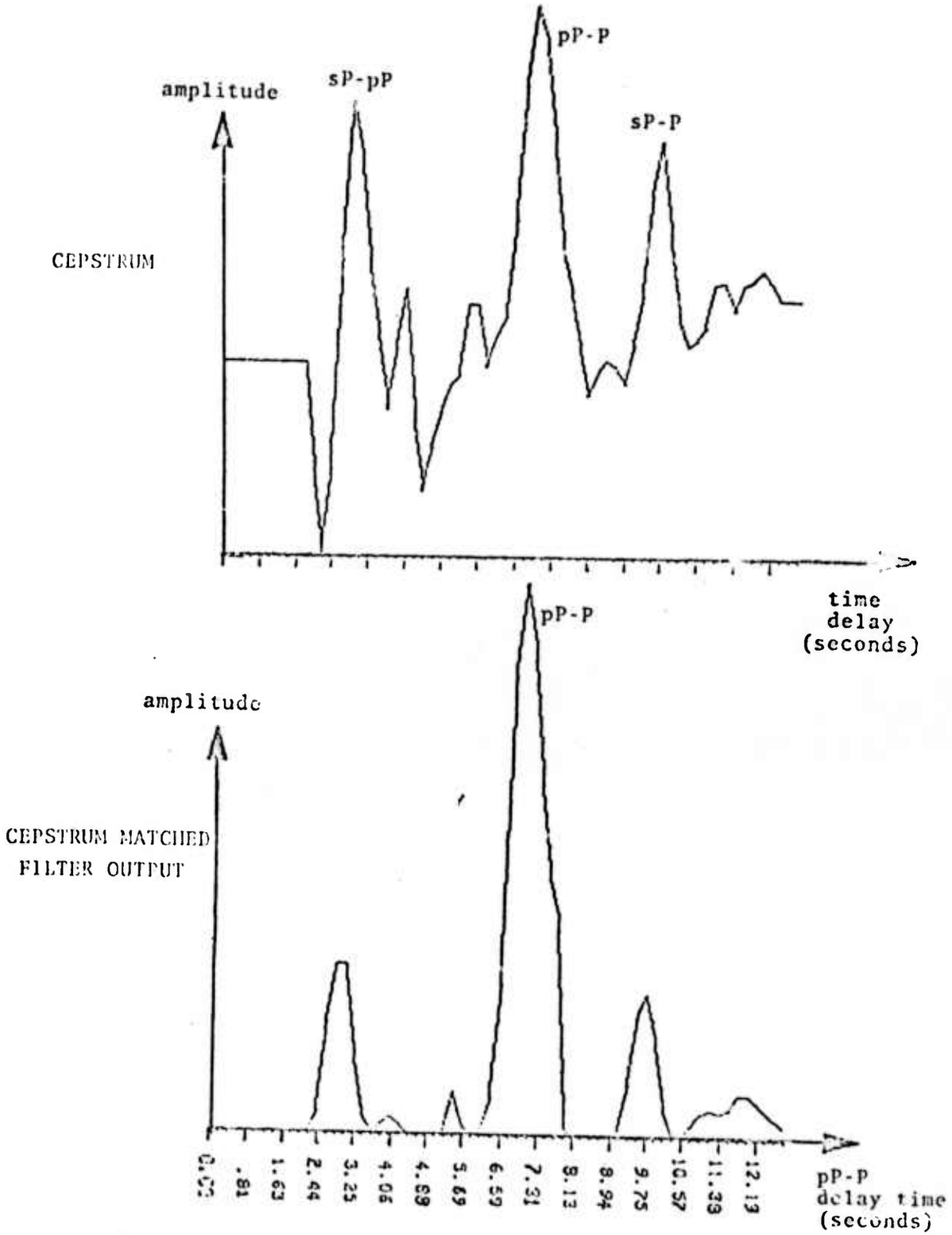

Figure 2. Cepstrum and Cepstrum Matched Filter output computed from data recorded at several stations for an event with well defined depth phases.

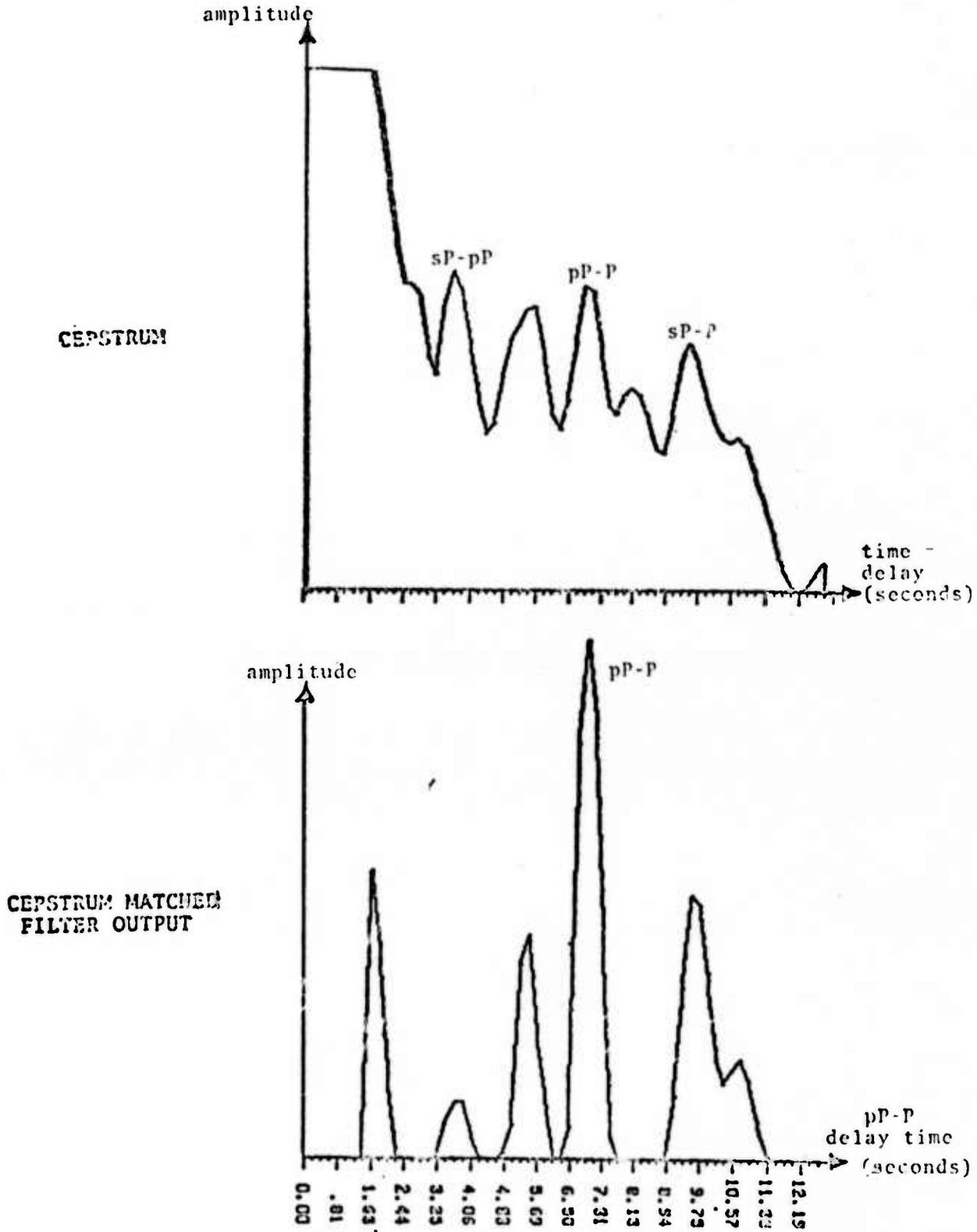

Figure 3. Cepstrum and Cepstrum Matched Filter output computed from data recorded at a single station for an event with well defined depth phases.

corresponding to the correct pP-P delay time. Additional examples showing the usefulness of the CMF technique in determining seismic source depths will be shown in Section 3.

2.3 Use of Seismic Travel Times To Account For Depth Phase Delay Time Variations Along The Coda

In the previous sections, we have discussed techniques which statistically allow for the variations in the differential delay times along the coda in order to enable more of the depth phase information to contribute to the depth phase detection. However, allowing for depth phase delay time variations through use of the Stochastic Cepstrum Stacking technique proves to be useful up to stochastic window widths of about 1 second. Events of interest to this work can have delay time variations of several seconds; for example (pP-P)-(pPP-PP) = 3.9 seconds for a depth of 50 kilometers and an epicentral distance of 30^{o}. The stochastic stacking technique could not encompass such variations without a severe loss in detectability and resolution, unless that portion of the coda containing the PP arrivals from the analysis is eliminated or some means is utilized to normalize this data to the direct phase.

In Figure 4, we show an illustration of such a case. Here, seismograms are depicted for recordings of an event at two stations. From the illustration, we see that the pP-P delay time is considerably larger than the pPP-PP delay time, and, therefore, the cepstrum peaks computed from samples 1 and 2 will not constructively average. The right side of Figure 4 illustrates that the peaks in the CMF output would also lie at different delay times and can not be constructively averaged in a linear sense. A similar situation is found with the data recorded at station 2, but here the delay times are, in addition, altered relative to station 1 by the station moveout. One would like to be able to combine the CMF outputs computed from the four samples in a manner which would allow these peaks to constructively reinforce at the pP-P delay time. This is shown at the bottom of the figure.

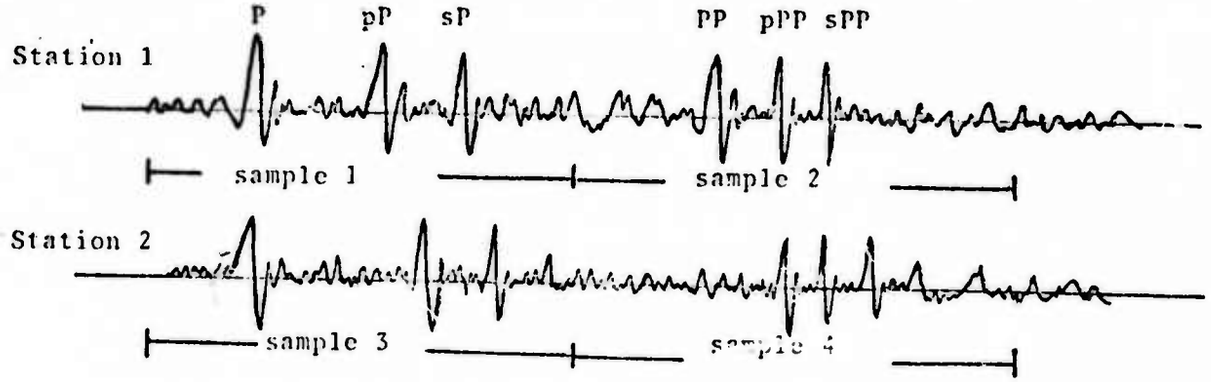

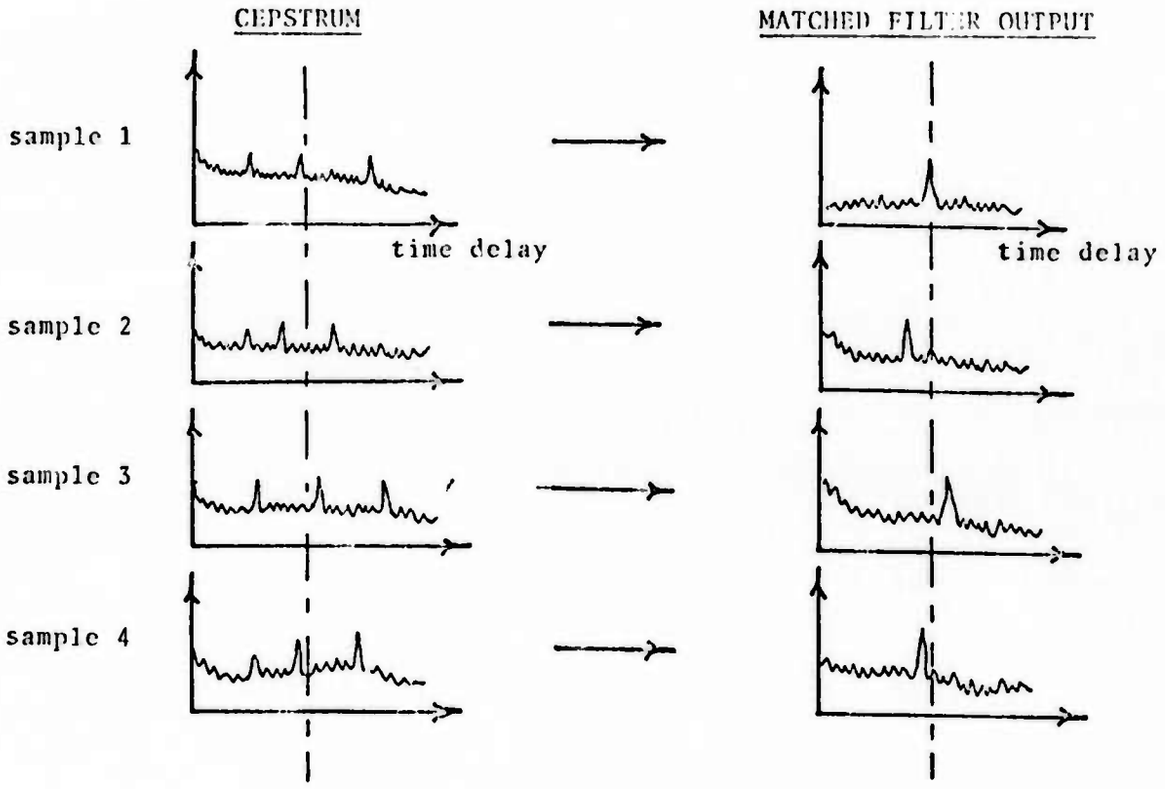

Combined Cepstrum Matched Filter outputs compensated for:

1. depth phase delay time differences of later phases.
2. station moveout

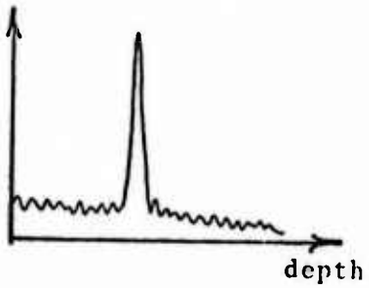

Figure 4

If one calculates the delay time variations expected along the coda for various event depths and distances using a seismic arrival time program, the appropriate delay time corrections could be applied to the CMF output of each sample before averaging. The degree to which the CMF output peaks stacked would then be a measure of how well the various depth phase delay times, computed along the coda and at different stations, all agreed with a given source depth assumption. Using such a procedure, all of the depth phase information contained in the seismogram would contribute to the depth phase detection.

In order to develop such a procedure one first needs the appropriate travel time information. Differential travel times such as sP-P, pPP-PP, sPP-PP. pPcP-PcP, sPcP-PcP, pPPP-PPP, and sPPP-PPP are not easily obtained from existing tabulations. These are the phases which comprise that portion of the seismic coda usually available for depth phase analysis. To determine these travel times, a ray tracing program based on the spherically symmetric isotropic earth velocity model used to calculate the BSSA (Bull.Seism. Soc. Amer., Vol. 58, No. 4(extract), August 1968) seismological tables for P phases was used . The program was checked by exactly reproducing selected travel times listed in the BSSA tables.

Figures 5, 6, and 7 give the computed time differences for the (pP-P)-(pPP-PP), (pP-P)-(pPPP-PPP), and (pPcP-PcP)-(pP-P) time delay differences. These charts give the expected shift of the CMF output peaks relative to the pP-P delay time, computed from portions of the coda containing either the PP, PPP, or PcP arrivals. One notes that these shifts are more significant for event depths greater than $\sim$ 10 km. Through use of these charts, cepstra or CMF outputs computed from different

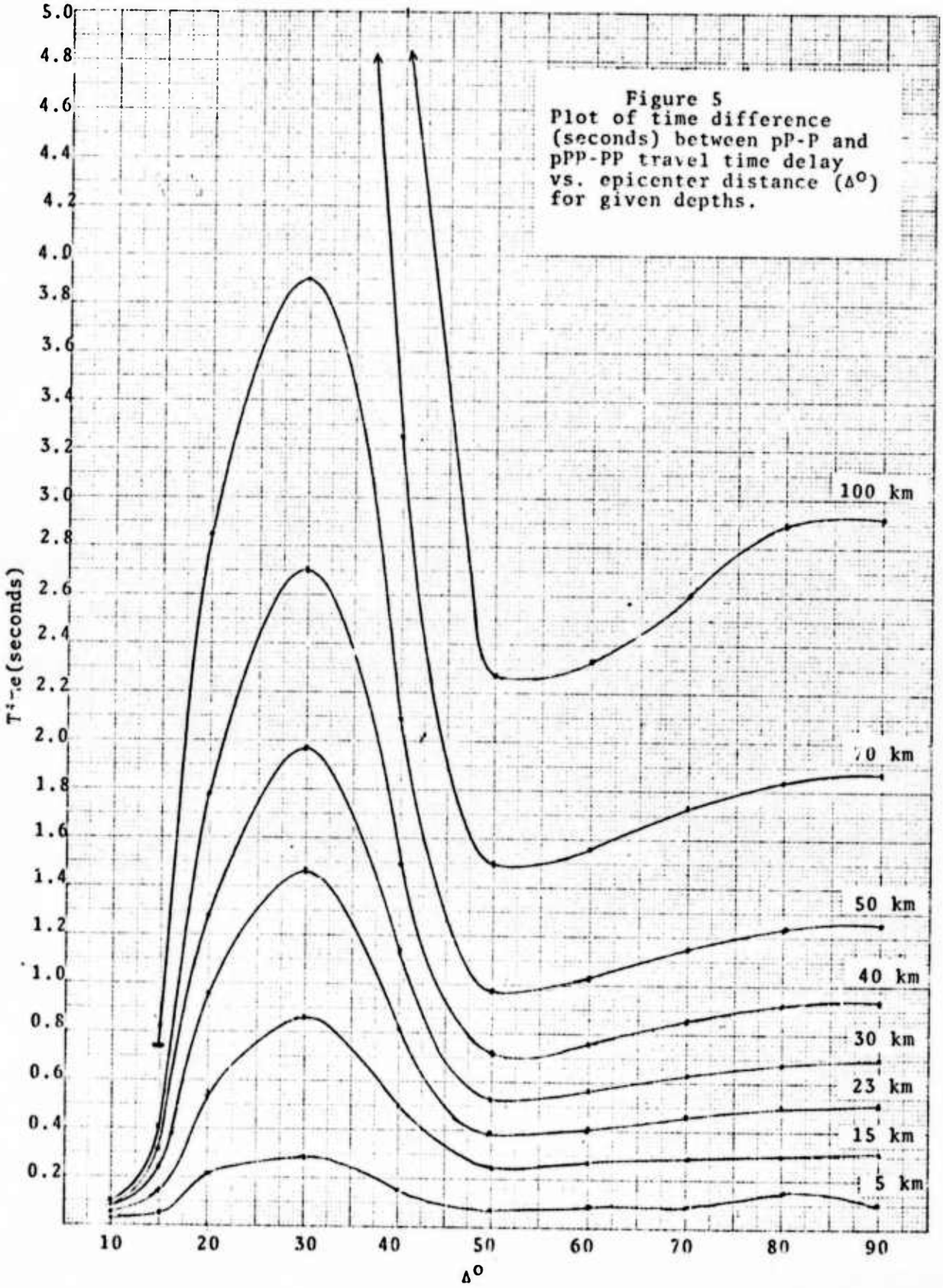
Figure 5
Plot of time difference (seconds) between pP-P and pPP-PP travel time delay vs. epicenter distance (Δ°) for given depths.
Time (seconds)
5.0
4.8
4.6
4.4
4.2
4.0
3.8
3.6
3.4
3.2
3.0
2.8
2.6
2.4
2.2
2.0
1.8
1.6
1.4
1.2
1.0
0.8
0.6
0.4
0.2
100 km
70 km
50 km
40 km
30 km
23 km
15 km
5 km
10
20
30
40
50
60
70
80
90
Δ°

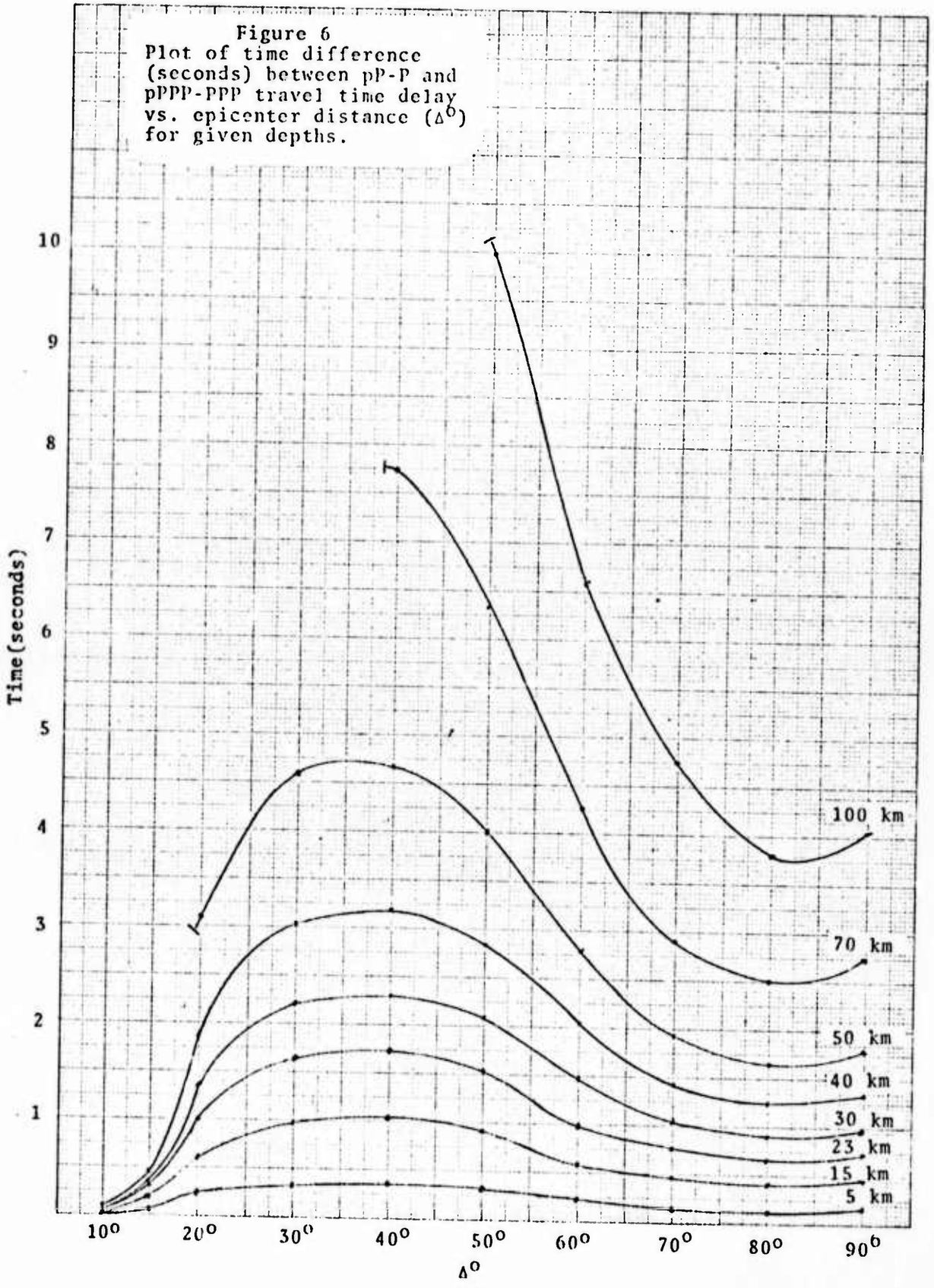

Figure 6
Plot of time difference (seconds) between pP-P and pPPP-PPP travel time delay vs. epicenter distance (Δ^{o}) for given depths.

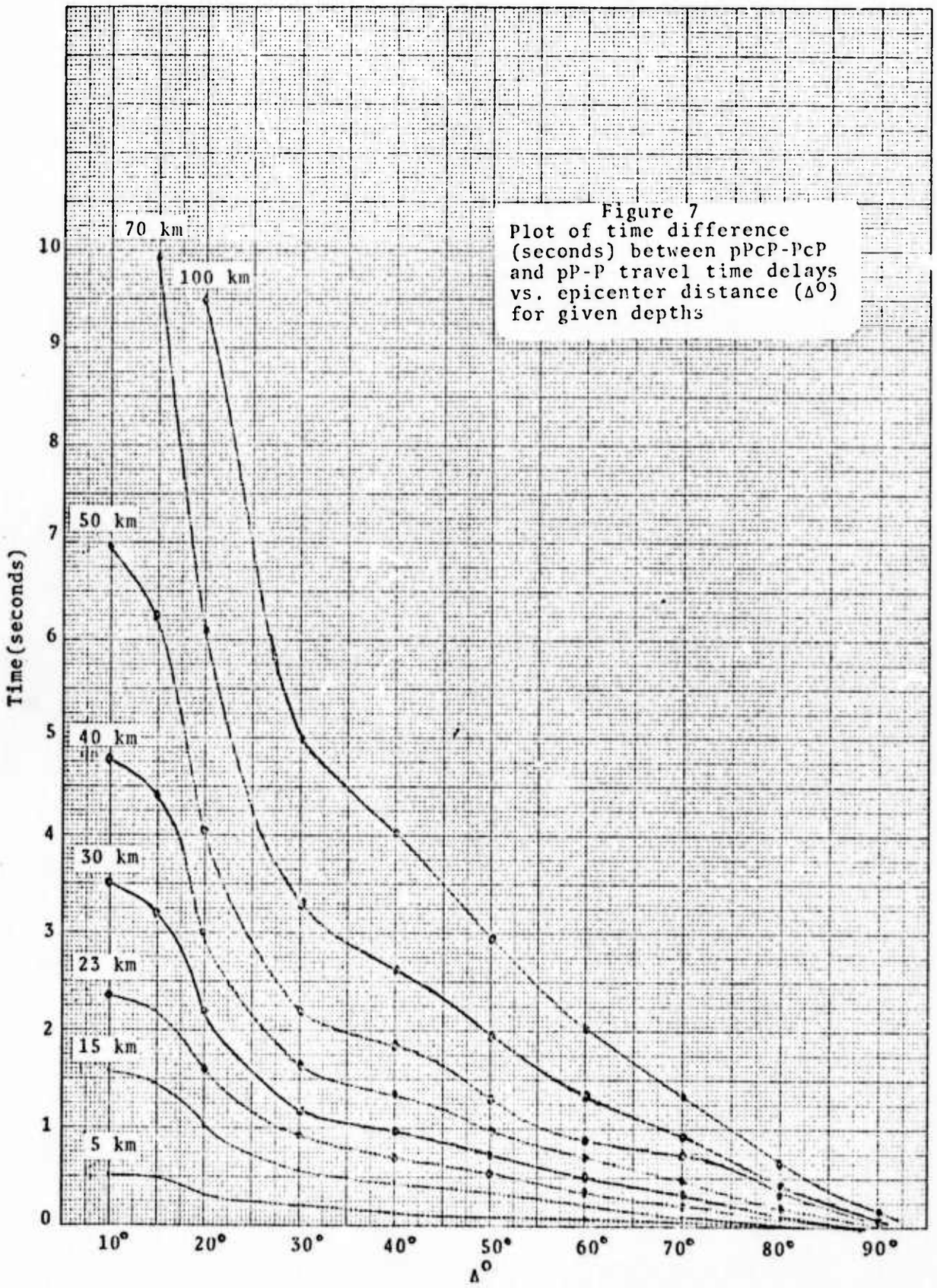

Figure 7
Plot of time difference (seconds) between pPcP-PcP and pP-P travel time delays vs. epicenter distance (Δ^{o}) for given depths

portions of the seismogram can be constructively averaged to produce a prominent peak at the pP-P delay time. Such a technique should prove very useful in improving both depth phase detection and depth phase delay time resolution.

The travel time differences for pPP-PP, pPcP-PcP, and pPPP-PPP are shown in Figures 8 and 9. In Figures 10 and 11 are shown plots of the pP-P delay times for the depths 5 to 40 km and 5 to 100 km respectively. In Figure 12, the PP-P, PcP-P, and PPP-P delay times for a range of depths and distances are given. The travel time differences plotted in Figure 12 can be represented by single curves for source depths between 5 and 100 km since the depth dependence turns out to be very weak. This points out that these phases alone are not useful for depth determination. The arrows in the figure indicate the minimum epicenter distance to which the PP, PPP, and PcP phase exists for given depths.

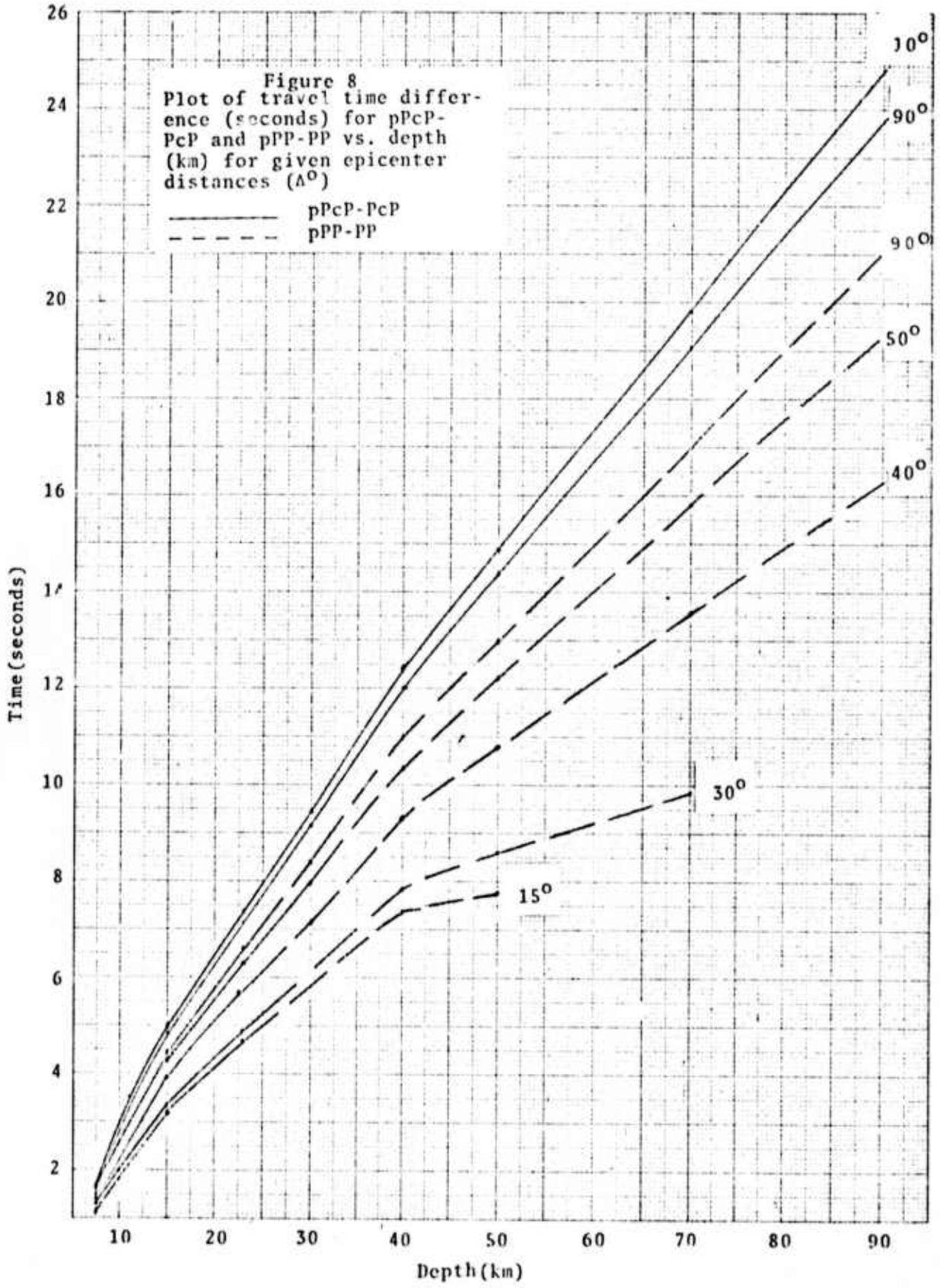
Figure 8
Plot of travel time difference (seconds) for pPcP-PcP and pPP-PP vs. depth (km) for given epicenter distances (Δ°)
pPcP-PcP
pPP-PP
10°
90°
90°
50°
40°
30°
15°
Time (seconds)
Depth (km)
2
4
6
8
10
12
16
18
20
22
24
26
10
20
30
40
50
60
70
80
90

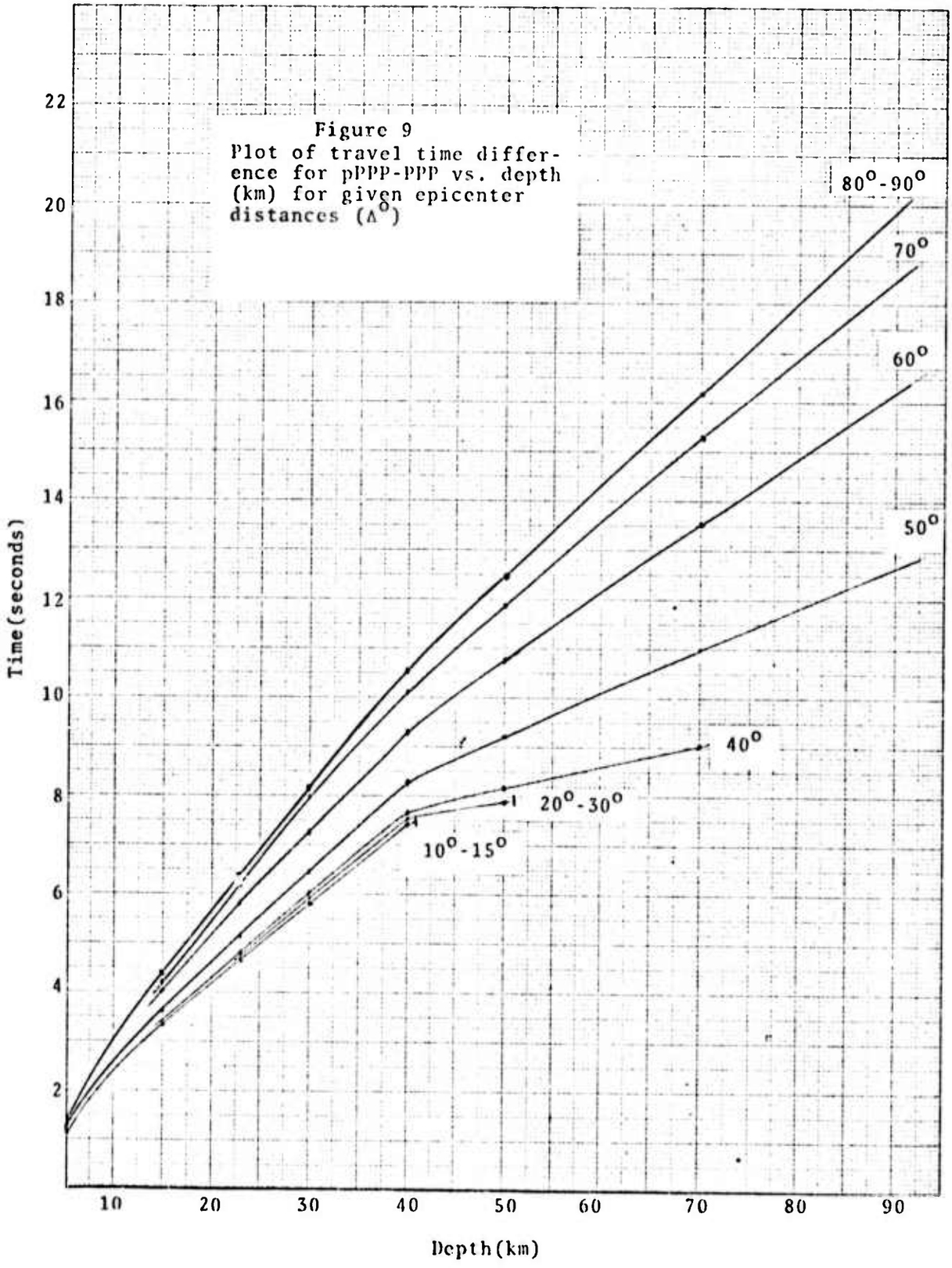
Figure 9
Plot of travel time difference for pPPP-PPP vs. depth (km) for given epicenter distances (Δ°)
80°-90°
70°
60°
50°
40°
20°-30°
10°-15°
Time (seconds)
Depth (km)
2
4
6
8
10
12
14
16
18
20
22
10
20
30
40
50
60
70
80
90

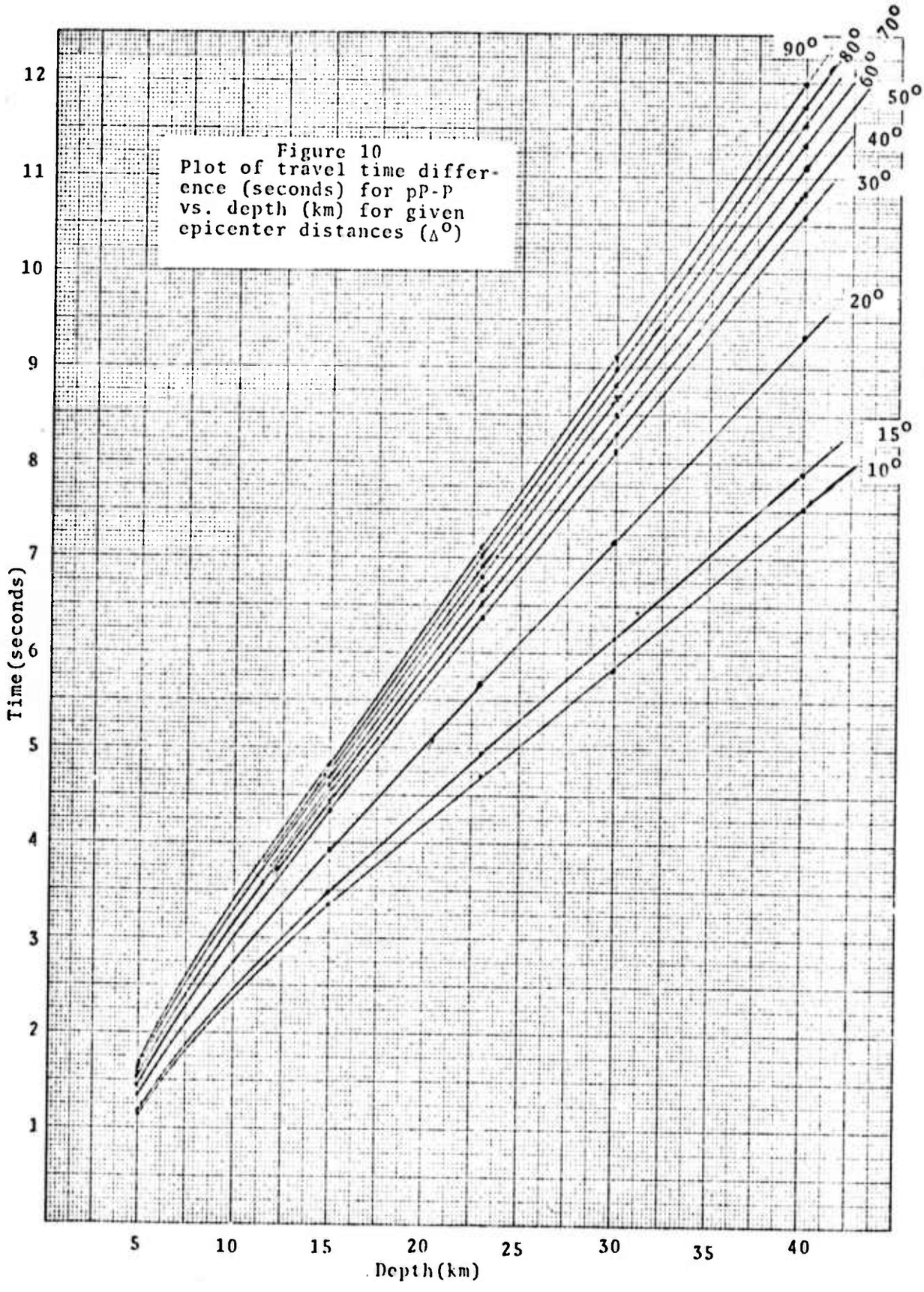

Figure 10
Plot of travel time difference (seconds) for pP-P vs. depth (km) for given epicenter distances (Δ^{o})

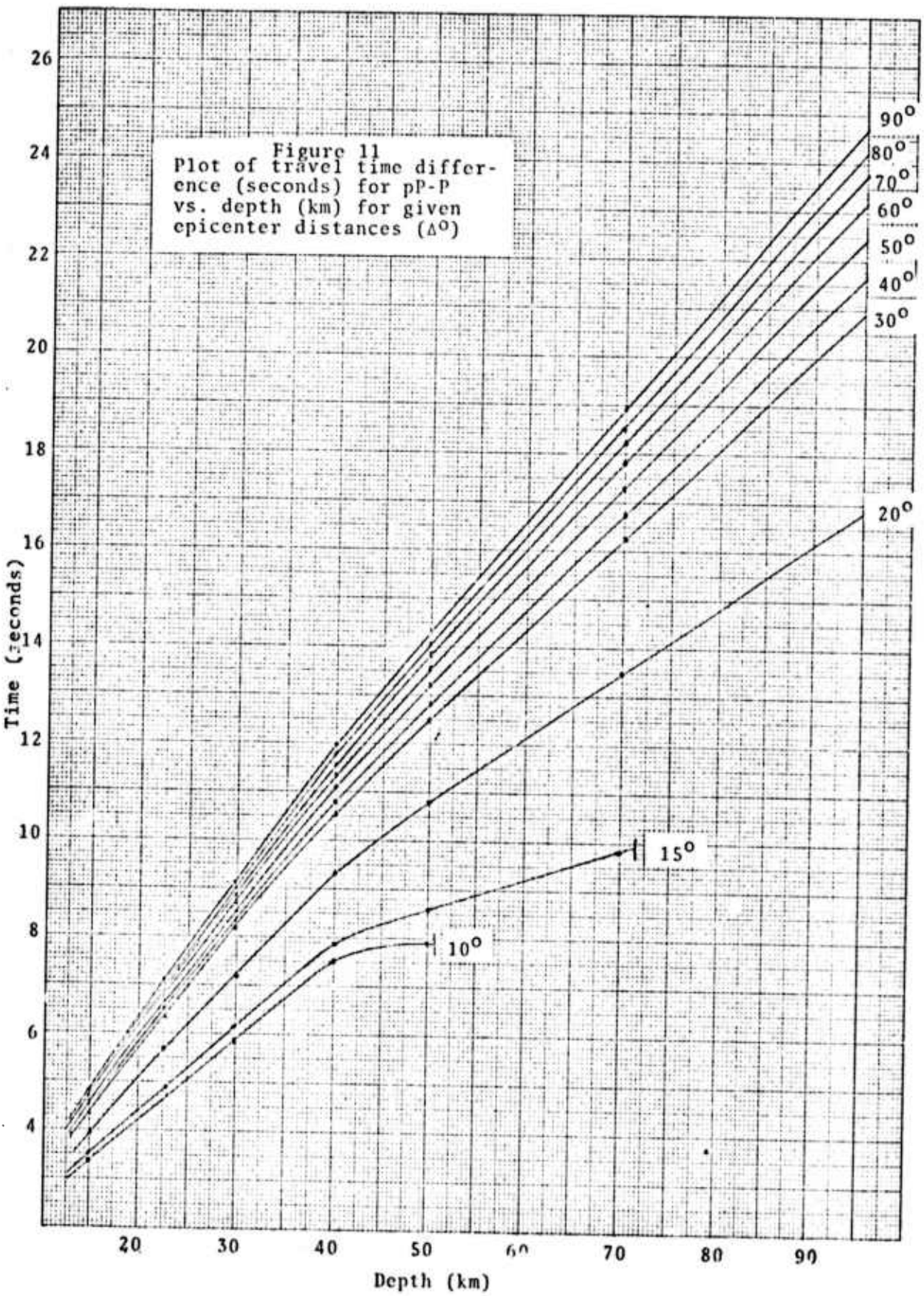
Figure 11
Plot of travel time difference (seconds) for pP-P vs. depth (km) for given epicenter distances (Δ°)
Time (seconds)
Depth (km)
90°
80°
70°
60°
50°
40°
30°
20°
15°
10°
26
24
22
20
18
16
14
12
10
8
6
4
20
30
40
50
60
70
80
90

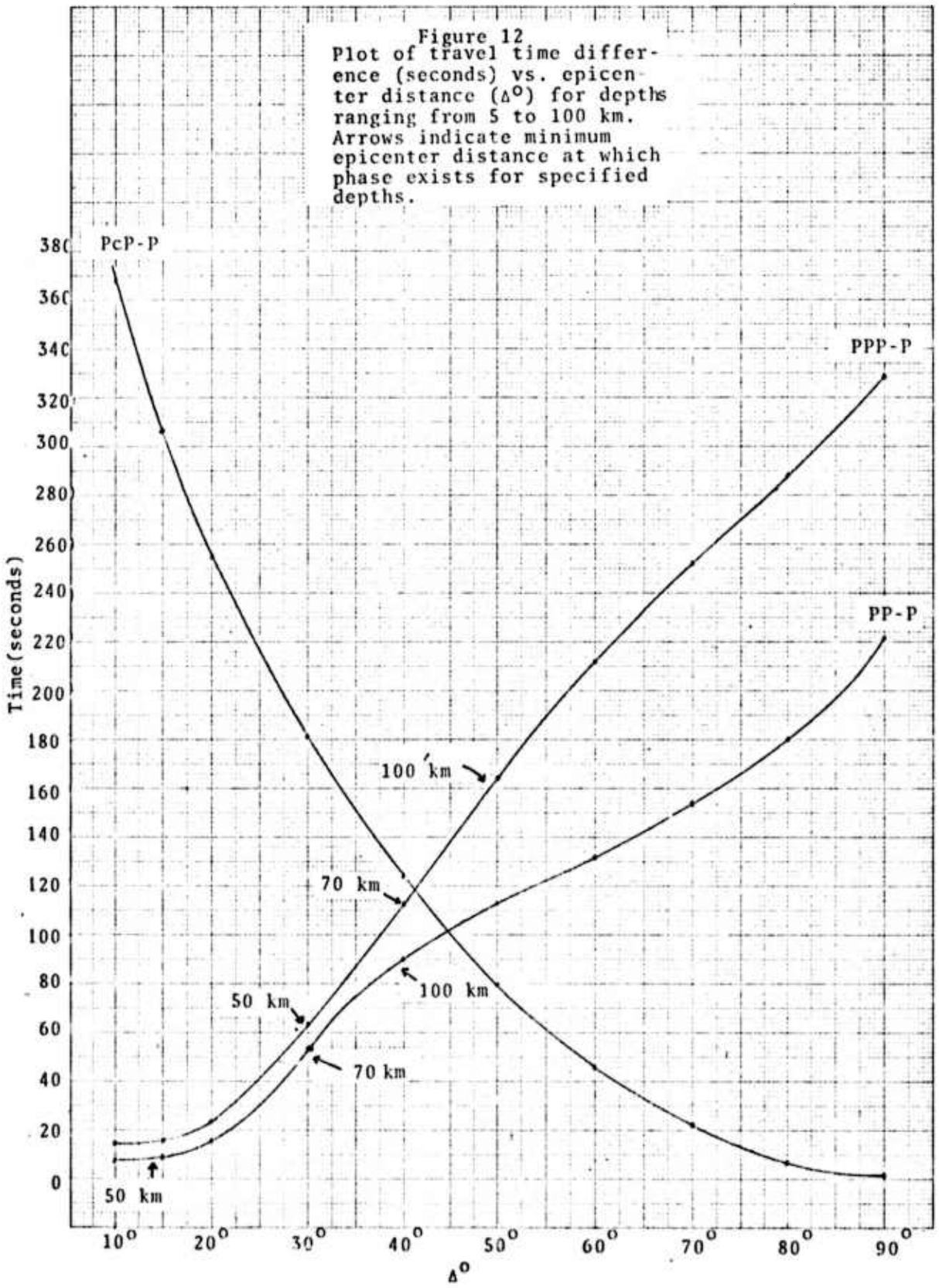

Figure 12
Plot of travel time difference (seconds) vs. epicenter distance (Δ^{o}) for depths ranging from 5 to 100 km. Arrows indicate minimum epicenter distance at which phase exists for specified depths.

3.0 APPLICATION OF THE NEW DEPTH PHASE DETECTION TECHNIQUES TO THREE SEISMIC EVENTS

Three seismic events, having known source depths, were chosen for analysis using the new depth phase detection techniques. These events had depths of 24, 178, and 53 kilometers and represent a range of signal to noise ratios such that visual identification of the depth phase is easy for one event, difficult for another and impossible for the third event.

3.1 Analysis of the Illinois Event

The Illinois Event of 11/9/68 was analyzed for differential travel time information using data recorded at six LRSM stations (KN-UT, MN-NV, PGZBC, WHZYK, FB-AK, NP-NT) at a 20 pts/sec. sample rate. This event was selected because the pP phase can be accurately identified from the seismograms (see Figure 13) and results obtained using the new techniques could be verified.

3.1.1 Evidence of Improved Depth Phase Detectability Using Seismic Coda

The analysis was carried out by first computing cepstrums using 14 consecutive 12.8 second data samples from each of the seismograms. (The same analysis was carried out using samples which overlapped by 25% and 50% and no significant changes in the results were noted.) Cepstrum phasors as well as the cepstrum amplitudes were computed using the steps described in Appendix C. In Figure 14 are plotted the cepstrum stacks

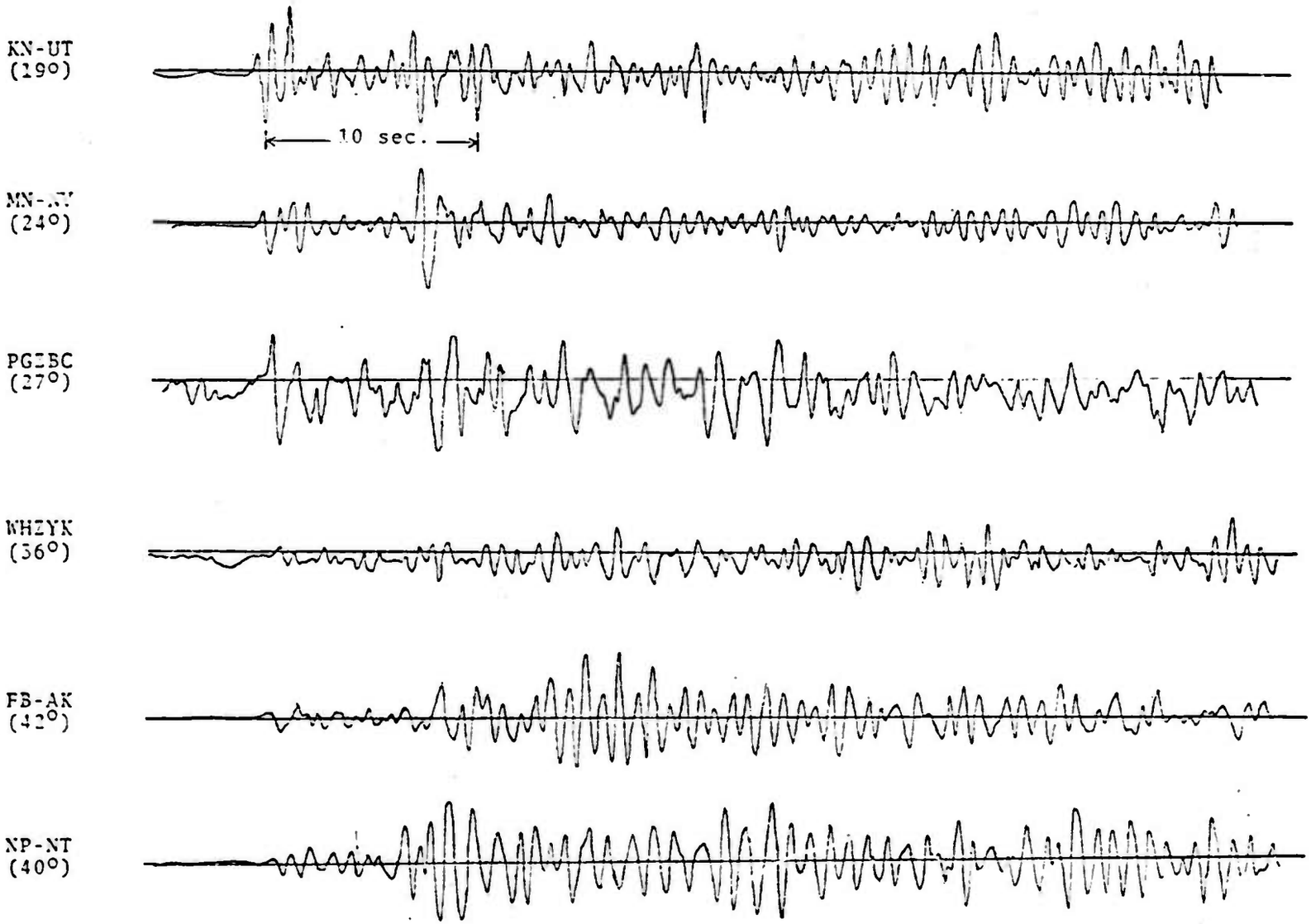

Figure 13. ILLINOIS EVENT 11/9/68

14a

CEPSTRUM STACK
(1ST - 12.8 SECOND SAMPLE FROM EACH STATION)

14b

CEPSTRUM STACK
(5 - 12.8 SECOND SAMPLES FROM EACH STATION)

14c

CEPSTRUM PHASOR STACK
(5 - 12.8 SECOND SAMPLES FROM EACH STATION)

14d

SYNTHETIC CEPSTRUM STACK
(τ_1 = 7.0; τ_2 = 10.0)

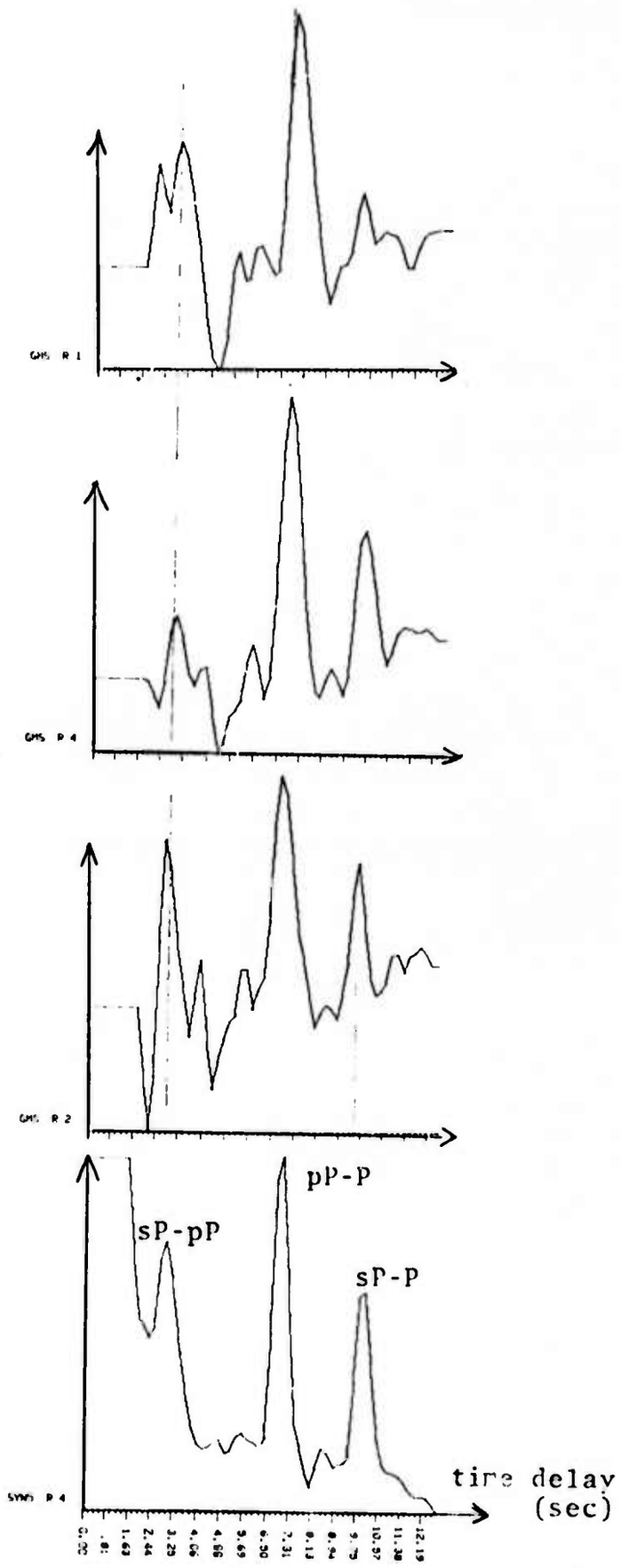

Figure 14. CEPSTRUM STACK FOR ILLINOIS EVENT

computed by averaging six cepstra calculated using the first 12.8 second data sample from each station (the start of these data samples was ∿ 1 second before the onset of the P-wave). There is a dominant peak at ∿6.8 second delay time corresponding to a pP-P delay time for a 24 km deep event recorded at approximately 30°. In Figures 14b and 14c, are the cepstrum stack and cepstrum phasor stack each calculated by averaging 30 cepstra computed using the first five 12.8 second samples from all six stations.

In both of these cepstrum stacks, a clear peak at ∿9.8 seconds has now emerged and corresponds to the known sP-P delay time for this event. This is evidence that improved depth phase detectability is obtainable by including data from the seismic coda in the analysis. Figure 14d is a plot of a cepstrum stack computed from data simulated to have pP-P and sP-P delay times of 7 and 10 seconds respectively. There is good agreement of this theoretical cepstrum result with those computed from the data. (Appendix D describes the steps used to generate the simulated seismogram.) Figure 15 shows the cepstra calculated for the individual stations used to record the Illinois Event.

Additional evidence that the coda contains usable depth phase information is obtained by analyzing a portion of the coda starting at 12.8 seconds from the onset of the P-wave. By eliminating the first 12.8 seconds of the seismogram and averaging five 12.8 second samples from each station, one still achieves clear detection of both the pP and sP depth phases as is shown in Figure 16.

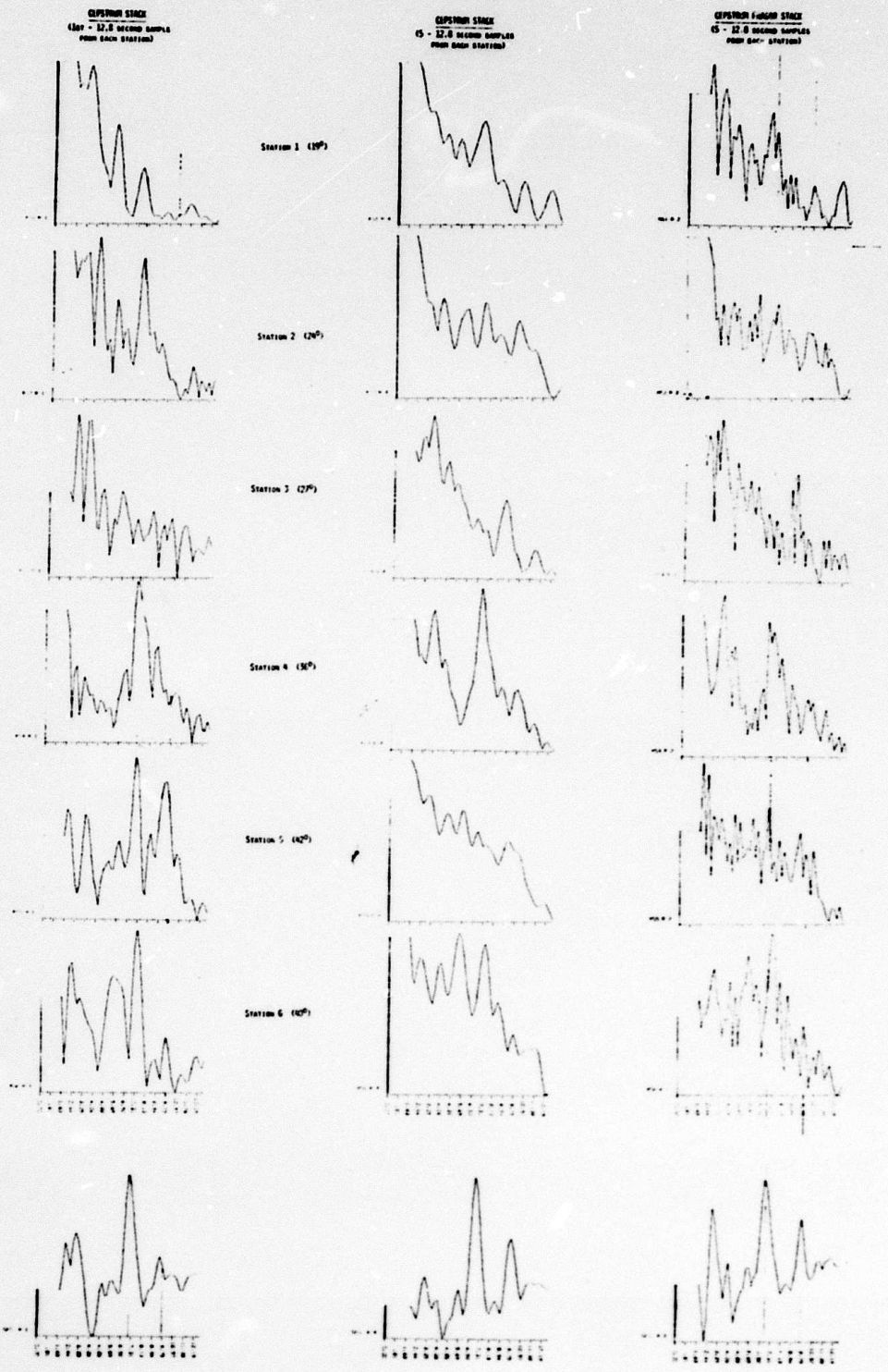

Figure 15. RESULTING CEPSTRUM STACKS FOR INDIVIDUAL STATIONS

USE OF SEISMIC CODA IN DEPTH PHASE DETECTION

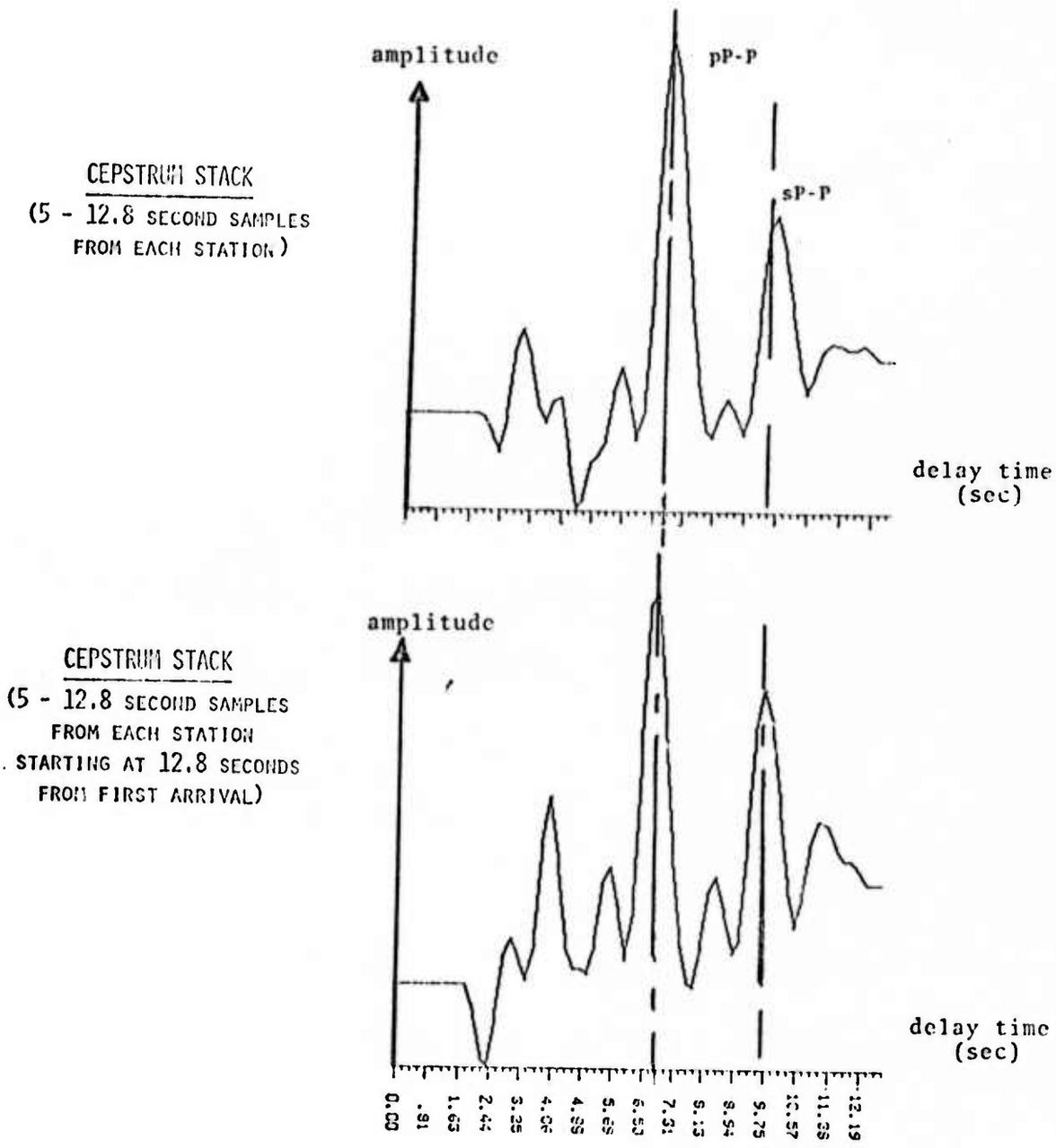

Figure 16. Cepstrums computed with and without the first arrival portion of the seismogram included.

3.1.2 Effect of Later Portions of the Coda on Detection

From the results presented in Figures 14 and 16, it is clear that depth phase information contained in the first minute of coda can be utilized to improve depth phase detection. However, by including the next 90 seconds of data in the analysis, detection is found to deteriorate because the differential delay times are substantially different in this portion of the coda. As was discussed in Section 2.3, one must deterministically account for the delay time variations associated with the later seismic arrivals when these variations are greater than $\sim$ 1 second. The results of using different portions of the coda for the analysis are shown in Figure 17. In Figure 17b is the cepstrum resulting from an analysis which included the first 3 minutes of the seismograms. This cepstrum does not have clearly defined peaks and is essentially the result of combining the cepstra calculated from the first minute of data (Figure 17a) with those calculated from the next 90 seconds of data (Figure 17c), the latter having dominant peaks at 4.9 and 7.8 seconds. The 4.9 second delay time is in agreement with the range of both the pPP-PP and pPPP-PPP delay times for a 24 km event recorded over a 20^{o} to 40^{o} range (see Figures 8 and 9.) From Figure 12 one notes that both the PP and PPP phases are present in the second minute of the seismogram for this event.

Thus, if one were to anticipate these delay time shifts for a given depth, one could then shift and average these cepstra such that they would reinforce at the pP-P delay time. This procedure would allow the depth phase information from more of the coda to contribute to the detection and avoid the deterioration of results

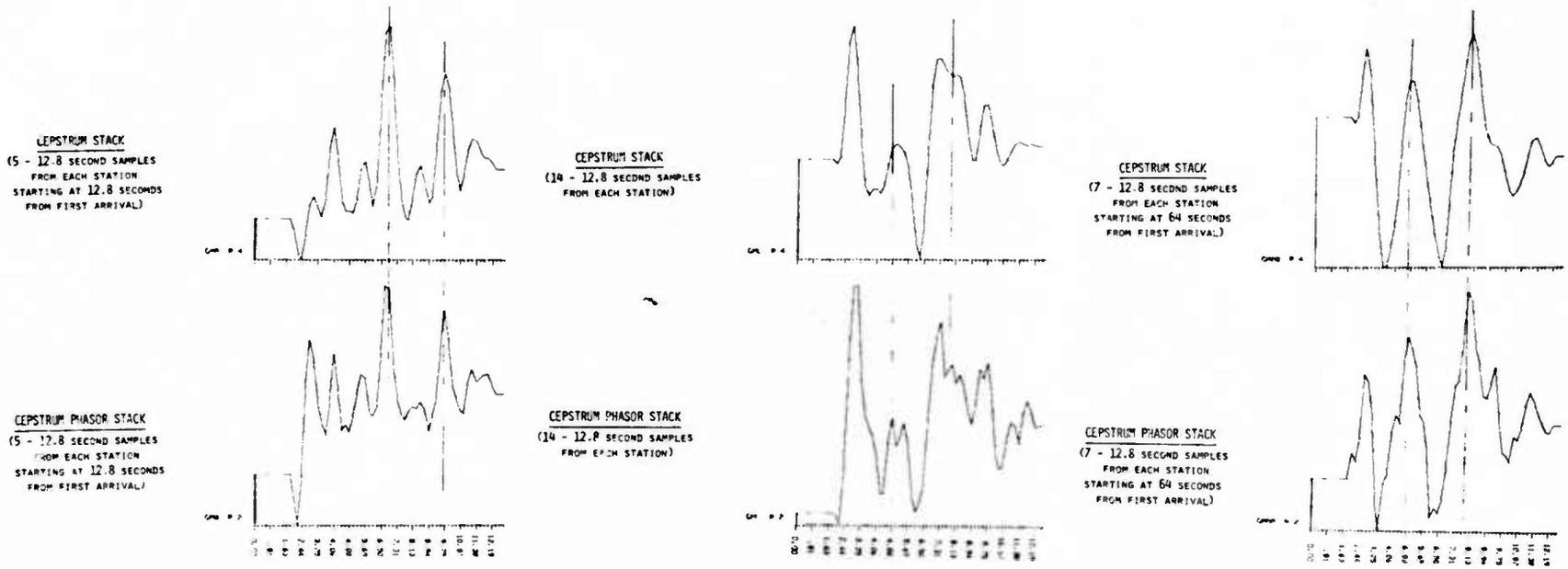

17a 17b 17c

Figure 17. CEPSTRUM STACK COMPUTED FROM VARIOUS PORTIONS OF THE CODA (TIME DELAY IN SECONDS)

occurring when the stochastic stacking window cannot absorb these large delay time variations. For the Illinois event, analysis must be restricted to the first 90 seconds of data if one does not apply a delay time compensation according to travel time information for the later phases.

3.1.3 Cepstrum Matched Filter Interpretation of Result

The results shown in Figures 14 and 16 indicate three dominant cepstrum peaks corresponding to the sP-pP, pP-P, sP-P delay times. In general it is difficult to determine the source depth from this information since the relationship among the peaks is not immediately apparent by visual inspection. An interpretation of these results can be substantially improved through use of the CMF technique discussed in Section 2.2. Figure 18 shows the resulting CMF output plotted with a seismogram recorded at KN-UT for the Illinois event. The CMF output shows a single dominant peak corresponding to the pP-P delay time for this event and is in agreement with the identification of the pP-P delay time observed in the seismogram. This result reflects the fact that all three cepstrum peaks arise from a single source depth having pP-P delay time of $\sim$ 6.8 seconds, averaged over the six stations. The CMF technique allows improved and automatic determination of the source depth from the computed cepstra.

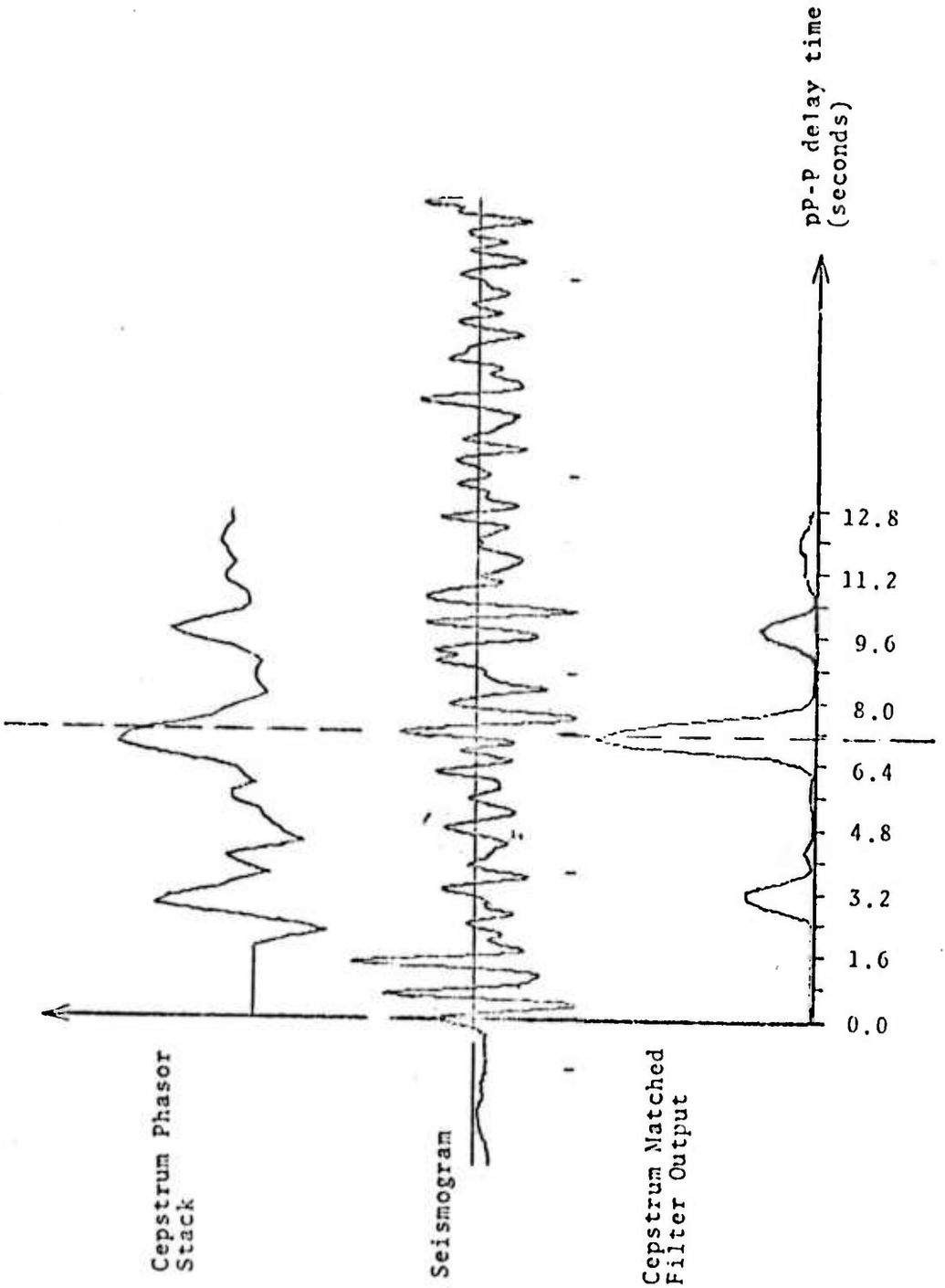

Figure 18. Cepstrum Phasor Stack, Seismogram, and CMF Output for Illinois Event.

3.2 Analysis of the Kamchatka Event

The Kamchatka event of 3/15/69 was next analyzed for the depth phase delay time using data recorded at 20 pts/sec at the four stations PIWY, RKON, DRCO, and LCNM. The first minute of the seismogram for this event is plotted in Figure 19. Cepstra were computed using the first 102.4 seconds of data recorded at each station (additional coda data was not available for this event). A stochastic cepstrum stack was then computed using stochastic windows ranging from 0 to 3 seconds. At the top of Figure 20 is plotted the stochastic cepstrum stack computed using a stochastic window of 2 seconds which gives rise to a significant improvement in detectability over conventional averaging techniques. The stochastic window served the purpose of allowing for delay time variations primarily associated with station moveout which was as large as 1.5 seconds for these recordings. In the analysis of the Illinois event the station moveout gave rise to a maximum delay time difference of $\sim$ .6 seconds and stochastic stacking gave an insignificant improvement in detectability over normal averaging. At the top of Figure 20, dominant peaks are observed at $\sim$ 14 seconds and at $\sim$ 42 seconds. To interpret this cepstrum pattern, the CMF technique was applied and the resulting output is plotted at the bottom of this figure. One again observes additional emphasis on the cepstral peak appearing at the correct pP-P time delay for this event which indicates a source depth of $\sim$ 178 km.

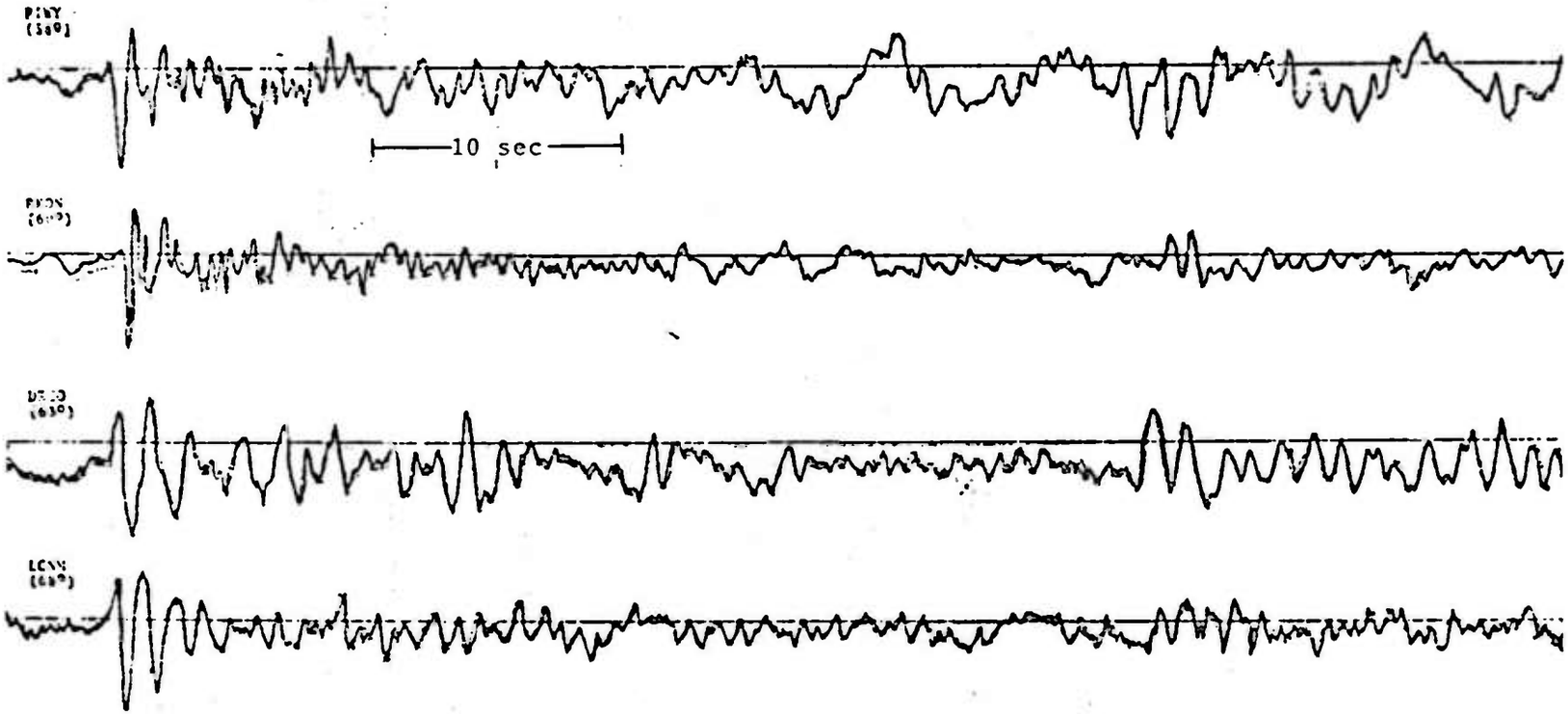

Figure 19. KAMCHATKA EVENT (3/15/69)

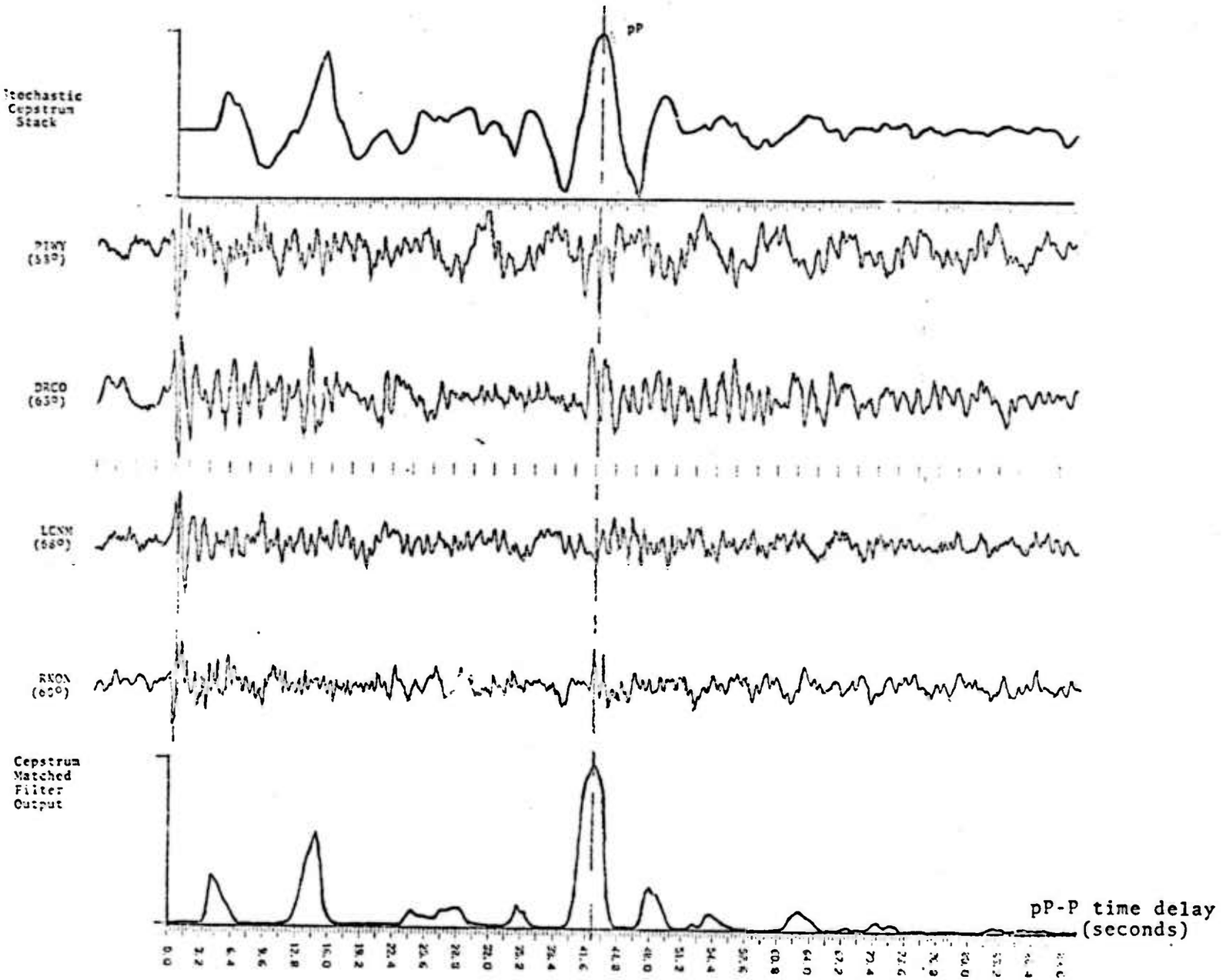

Figure 20. KAMCHATKA EVENT (3/15/69)

3.3 Analysis of the China Event

The third seismic event analyzed for depth phase information using the new techniques was the China Event of 6/5/64. This event was analyzed using data recorded at 20 pts/sec at the three stations GG-GR, BMO, and UGO. As is seen in Figure 21, the recordings have very poor signal to noise ratios, and it is impossible for an analyst to determine the depth phase delay times visually. For this event, 9 cepstra were computed from the first three consecutive 25.6 second samples for each of the three stations. These cepstra were stochastically averaged using a stochastic window width of $\sim$ 1 second, and the stochastic cepstrum stack was computed using both the cepstrum and cepstrum phasor techniques. The cepstrum phasor technique gave somewhat better results in this case and is plotted at the top of Figure 22. Two cepstrum peaks stand out at $\sim$ 7 and $\sim$ 14 seconds but are not very convincing. However, by applying the CMF to this data, a more distinct peak appears in the CMF output at the correct pP-P delay time for this event (Figure 22, bottom). This peak appears at $\sim$ 14 seconds and corresponds to an event depth of $\sim$ 53 km for these source to station distances. This result gives a striking example of the ability of these new techniques to detect the depth phase and obtain accurate source depth estimates from recordings of events in which conventional analysis would fail.

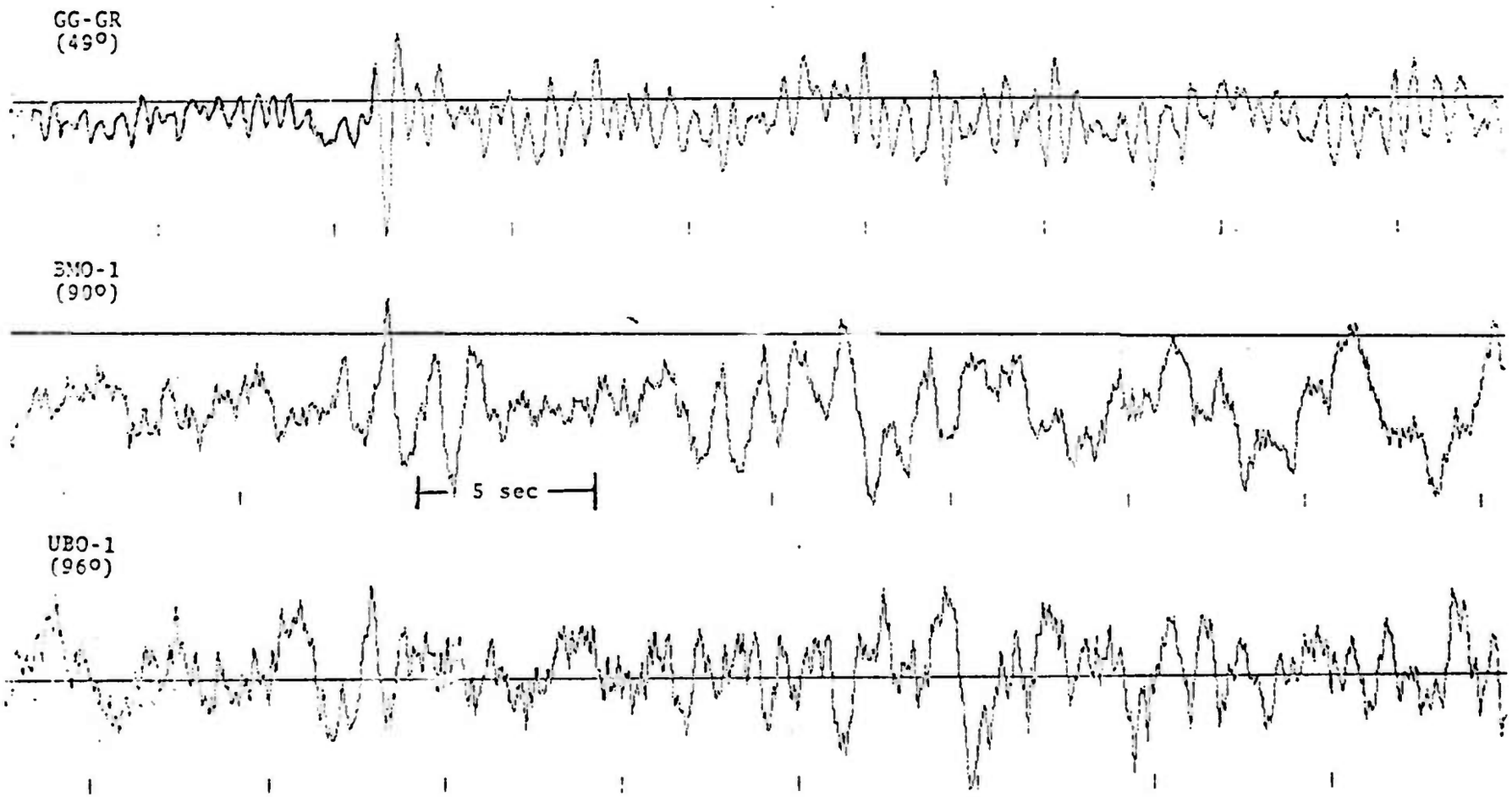

Figure 21. CHINA EVENT (6/5/64)

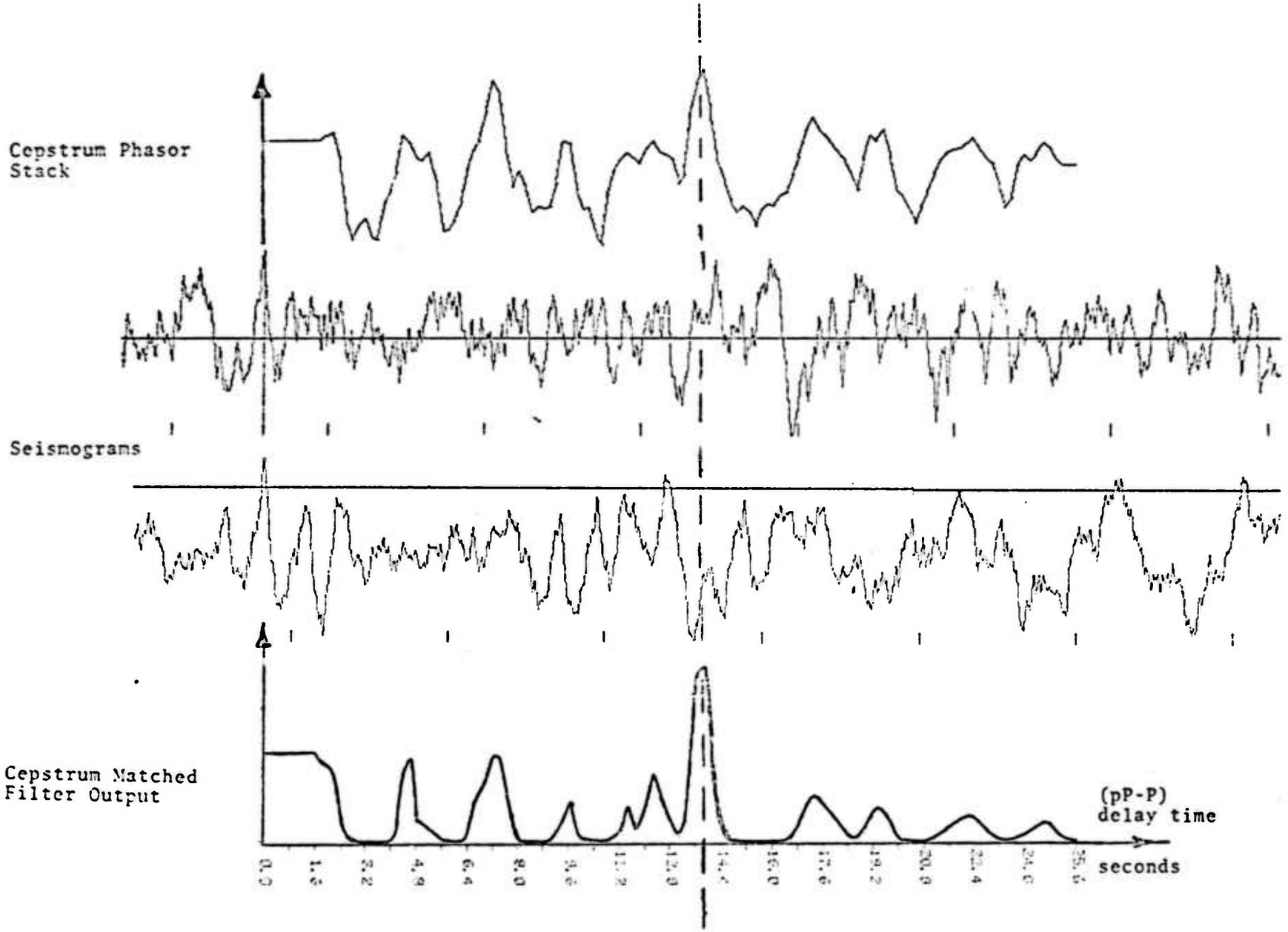

Figure 22. CHINA EVENT (6/5/64)

4.0 CONCLUSION

During this research effort, new seismic depth detection techniques have been investigated to determine whether they could significantly enhance one's ability to obtain accurate source depths at teleseismic distances. Three seismic events, each having well established depths, were analyzed using these techniques and clear detections of the correct pP-P delay times were obtained in each case. For at least one of these events, conventional depth phase analysis was not capable of obtaining a source depth estimate using the data analyzed in this work. Results of the research demonstrated that these new techniques represent a major improvement over conventional depth phase detection procedures through advances in both the detection and interpretation of seismic depth phase information. The new analysis method involved techniques which utilize more of the seismic depth phase information contained in the seismogram and techniques which also interpret the typically complicated cepstrum patterns to extract source depth estimates.

These techniques could next be incorporated in a seismic depth phase analysis package which would be of valuable assistance to the analyst. Such a package would automatically analyze the seismic data to extract accurate source depth estimates by determining the degree to which the cepstrum patterns, computed from different portions of the seismograms recorded over a suite of stations, agreed with those expected for a given event depth. This analysis would automatically make constructive use of depth phase information contained throughout the seismograms and should give the analyst the ability to determine accurate source depth estimates for a significantly larger percentage of events then is presently possible.

APPENDIX A
STOCHASTIC CEPSTRUM STACKING

A stochastic stacking technique can be used to increase the detectability of a peak whose position can vary unpredictably within a certain limited range. Consider a set of cepstrums calculated from consecutive time segments of a seismogram. If the depth phase delay time were the same in each segment, then by stacking (adding) these cepstrums, the amplitudes of the stationary peaks would constructively add, whereas the non-stationary peaks arising from origins other than the depth phase delay times would average to some lesser amplitude level. This is also true for the single cepstrum estimate using the entire seismogram.

By redefining the N cepstrum values x_i, i = 1,N to be

$$y_i = \text{MAX}\ (x_j,\ j=i - \Delta/2,\ j=i + \Delta/2)\ ,$$

for each point i, and then by adding the y arrays one can increase the detectability for cases in which the peak of interest moves unpredictably within a window Δ. Figure A-1 illustrates this technique using synthetic data. Each of the top six arrays are constructed of random numbers having amplitude values between 0 and 1. A peak (indicated by an arrow in the figure), defined by three points having amplitude values .8, 1.2 and .8,

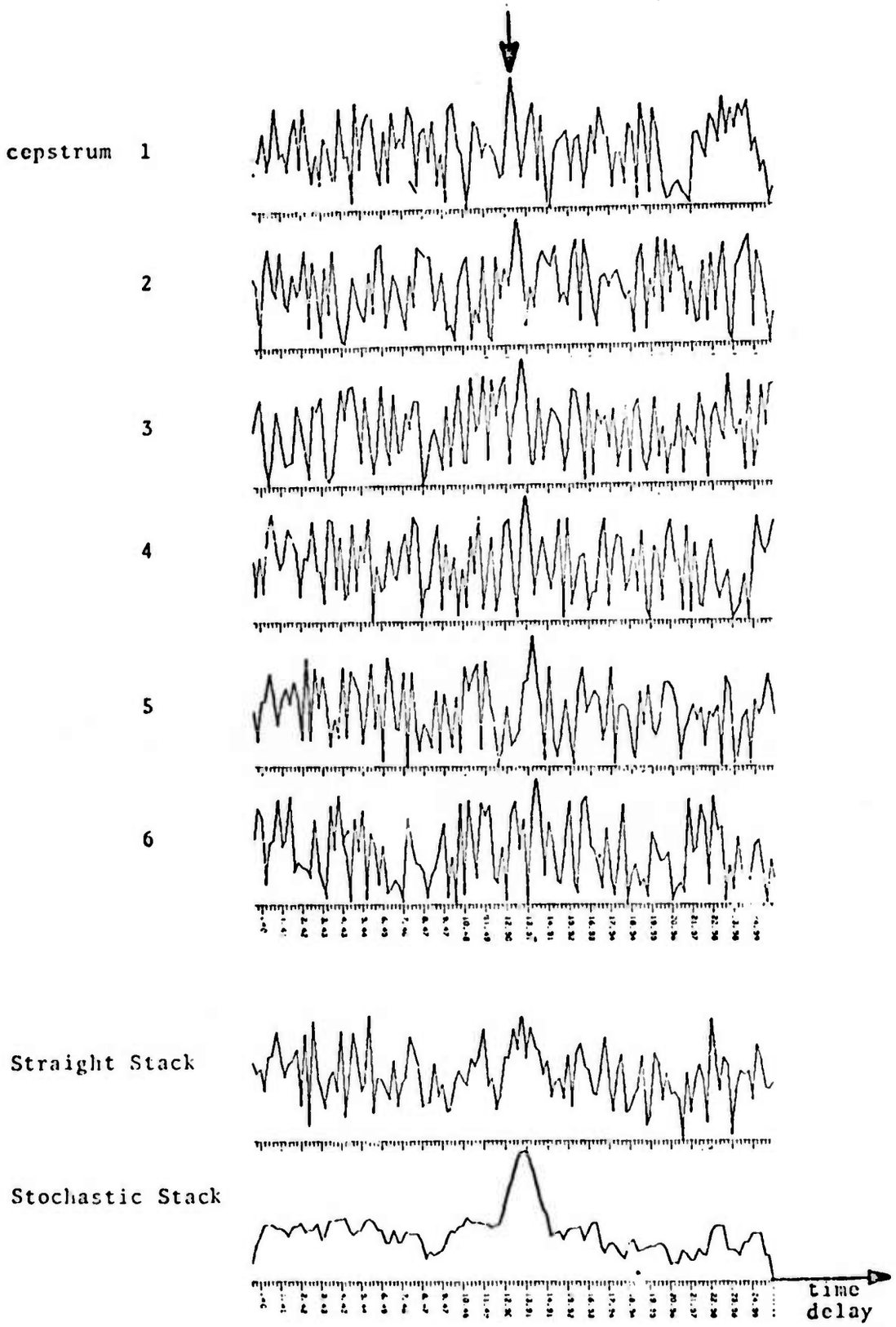

Figure A-1. Demonstration of Stocastic Stacking using Synthetic Data

is added to each of the six arrays, but shifted an additional point to the right in each consecutive array. The result of adding these arrays (Straight Stack) is shown, and it is seen that a clear detection of the peak is not achieved by ordinary stacking. However, if before adding, one redefines these arrays as has been outlined, the results (Stochastic Stack) show that a dramatic improvement in peak detection is achieved through the use of this stochastic stacking procedure.

Thus, the stochastic stacking technique can allow for the random or unpredictable variations in the seismic delay times which are not accounted for when using travel time information.

APPENDIX B
STOCHASTIC CEPSTRUM PHASOR STACK

Impressive improvements in seismic depth phase detection, in addition to those gained by stochastic stacking, have been obtained by using information concerning the phase difference between the direct and surface reflected seismic arrivals. To see how this can be achieved consider the steps involved in calculating a cepstrum.

Assume the received signal F(t) to be the sum of the direct wave f(t) and a single reflection of relative amplitude α, "phase" θ, and delay time τ. F(t) can be written

$$F(t) = f(t) + \alpha \, [f(t-\tau) \cos \theta + f_H(t-\tau) \sin \theta].$$

Here f_H represents the Hilbert transformation of f which corresponds to shifting each Fourier component of f by $\pi/2$. The bracketed expression then represents the signal f(t) having each of its Fourier components shifted by θ. This phase shift θ is the phase difference between the direct and reflected signal. For example, if the reflected waveform differed from the direct signal by only a change in sign, θ would equal π.

The power spectrum of F(t) is

$$P(\omega) = p(\omega)\ [1 + \alpha^2 + 2\alpha \cos\ (\omega\tau - \theta)],$$

for $\omega \geq 0$ and with $p(\omega)$ being the power spectrum of $f(t)$. As can be seen from the expression for $P(\omega)$, the power spectrum $p(\omega)$ is modulated by a cosinusoidal function having frequency τ and phase θ. Taking the complex spectrum of $P(\omega)$ one would then obtain a peak at lag τ having phase θ. Therefore, one can assign a phase θ to each point of the cepstrum calculated by taking the power spectrum of log $P(\omega)$.

To see how this phase information can aid in depth phase detection, consider events at $\leq$ 40 km. Here the direct and surface reflected seismic arrivals travel similiar paths once outside the vicinity of the event. It is then reasonable to assume that both the direct and surface reflected arrivals would undergo similar reflections, refractions, distortions, etc., once away from the source region and that the phase relationship established in the vicinity of the source should be unchanged at the receiver. If one considers those portions of the seismogram comprised entirely from P, pP and sP arrivals, then the phase angle associated with the cepstral peaks resulting from the presence of the pP and sP phases, would be similar in all such portions. Other cepstral peaks resulting from noise, etc., would tend to have more random phase angle over these portions of the coda. Thus by treating each cepstrum point as a phasor and adding the cepstrums vectorially we can enhance the detection of the depth phases. Later portions of the coda, resulting from other seismic phases (PcP, PP, etc.) can also be included in this cepstrum phasor stack if the phase

difference between P and pP is the same as the phase difference between the later phases and their associated surface reflected arrivals with π degrees.

These assumptions are really just generalizations of ideas normally assumed about the direct and reflected waves. It is common to consider the surface reflected arrivals to have a waveform similar to the direct arrivals but having the same or different sign depending on the angle of reflection and on the signs of the parts of the radiation pattern that radiate the direct and the reflected waves. This is equivalent to saying there is a 0 or π phase difference between the direct and reflected waves. What we have done is to generalize this idea to include all phase shifts, possibly arising from reflection, refraction or complex source radiation pattern) from 0 to 2π rather than just 0 and π and to use the consistence of $\theta \pm \pi$ throughout the seismogram to aid the depth phase detection. The usefulness of this technique has already been demonstrated in our work thus far.

APPENDIX C
CALCULATION OF THE STOCHASTIC CEPSTRUM STACK AND STOCHASTIC CEPSTRUM PHASOR STACK

The following steps are used to calculate the Stochastic Cepstrum Stack and Stochastic Cepstrum Phasor Stack for a seismogram consisting of NS consecutive portions each having N amplitude values:

- Select N sampled (sample rate = 20 pts/sec) amplitude values from the M^{th} portion of a seismogram

  $X_M(n)$, n=0, 1, ..., N-1

  and add N zeroes to interpolate the spectrum

- Calculate the amplitude spectrum for positive frequencies using

$$A_M(j) = \left| \frac{1}{2N} \sum_{n=0}^{2N-1} X_M(n) e^{-2\pi inj/2N} \right| ; \; j=0,1,\ldots, N-1$$

  with the Nyquist frequency = 10 Hz and $i = (-1)^{1/2}$.

- Retain only the lower quarter frequencies of the amplitude spectrum since there is very little energy at frequencies above 2.5 Hz for natural events. This leaves the array

$$(A_M(j),\ j = 0, 1, \ldots, N/4-1)$$

- Remove the mean and apply a cosinusoidal taper to the first 10% and last 20% of the A_M array giving the modified array

$$(A_M'(j),\ j = 0, 1, \ldots, N/4-1)$$

The 20% taper on the higher frequencies was used to de-emphasize the higher frequencies

- Add N/4 zeroes to interpolate the cepstrum giving the array

$$(A_M'(j),\ j = 0, 1, \ldots, N/2-1)$$

At this stage one would take the log of this A_M' array to obtain the log cepstrum; but by not using the log better results were obtained.

- Calculate the Fourier Transform of the A_M' array using

$$F_M(k) = \frac{1}{N/2} \sum_{j=0}^{N/2-1} A_M'(j) e^{-2\pi ijk/(N/2)}$$

where $(F_M(k), k = 0, 1, \ldots, N/4-1)$ are

complex numbers representing the positive frequency spectrum of A_M. One can now obtain the amplitude and phase of each cepstrum point k. The array

$(|F_M(k)|, k = 0, 1, \ldots, N/4-1)$ is what we

is referred to as the cepstrum amplitude and the complex numbers $F_M(k)$ are referred to as cepstrum phasors.

- To calculate the stochastic cepstrum stack, one then calculates

$$|F_M(k)| = \text{Max} (|F_M(j)|, j = k-\Delta/2, k+\Delta/2)$$

for each section M and sums these over the number of sections (NS) used from a given seismogram (Δ is the stochastic window width). This gives

$$C(k) = \sum_{M=1}^{NS} |F_M(k)| \cdot W_M \quad ,$$

where C(k) is the stochastic cepstrum stack and W_M is a weighting factor, chosen such that the mean amplitude of each $|F_M(k)|$ array is equal.

- To calculate the stochastic cepstrum phasor stack, each $F_M(k)$ is replaced by $F_M(n)$ where n is the index of the Max value of $|F_M(j)|$ in the interval $j=k-\Delta/2,\ k+\Delta/2$. The stochastic cepstrum phasor stack is then defined by

$$CP(k)=\left| \sum_{M=1}^{NS} W_M \cdot F_M(k) \right| \quad .$$

APPENDIX D

SYNTHETIC SEISMOGRAMS

Synthetic seismograms are generated by passing white noise through a recursive digital filter having a band pass typical for seismic arrivals and adding this signal to itself at delays τ_1 and τ_2 (corresponding to pP-P and sP-p time delays). The recursive digital filter was designed from the following z-transform of a resonator with poles at $z=r\exp(\pm j\omega_r T)$ and a zero at q:

$$H(z) = \frac{1-qz^{-1}}{(1-2r(\cos\omega_r T)z^{-1} + r^2 z^{-2})}$$

For q=1 this gives zero gain at $\omega=0$ and a resonant response with ω_r determining the resónant frequency and r relating to the Q of the response. We used q=1, r=.9 and $\omega_r=2\pi$ for the generation of the synthetic data with T being the inverse of the sample rate.